CHIRAL PERTURBATION THEORY AND THE WEAK INTERACTION

Thesis by

Johan Bijnens

In Partial Fulfillment of the Requirements

for the Degree of

Doctor of Philosophy

California Institute of Technology

Pasadena, California.

1985

(Submitted May 20, 1985)

dedicated to my parents

ACKNOWLEDGEMENTS

I sincerely thank my advisor Professor Mark B. Wise for all the help and encouragement he has given me. I would also like to thank him for being a most pleasant collaborator in the course of most of the work presented in this thesis.

Special thanks go to my office mate and collaborator Hidenori Sonoda and to Professors John Preskill, David Politzer and to Benjamin Grinstein for all the interesting and stimulating discussions about physics.

I would also like to express my gratitude to Walter Troost for constant advice and encouragement and for introducing me to the world of Particle Physics.

And last, my sincerest thanks to all those without whom life wouldn't have been the same: Howard Stone, Alexios Polychronakos and Paul Stolorz.

ABSTRACT

We study the interface between the standard six-quark model and the observed low-energy weak phenomena. The main processes discussed are weak decays of kaons and hyperons. We study first the low-energy effective weak Hamiltonian at the quark level. This is derived using the renormalization group in leading logarithmic approximation.

Then some properties of this effective weak Hamiltonian that can be derived using chiral perturbation theory are studied. A review of chiral perturbation theory is included.

This formalism is used to study the relation between $\bar{K}^0 K^0$ mixing and a $\Delta I=3/2$ decay. We find that the logarithmic corrections to this relation are large, making it unreliable. The same formalism is used to discuss a relation between $K\pi\pi$, $K\pi$ and K-vacuum matrix elements used in most attempts to compute the $K\pi\pi$ matrix element relevant for the $\Delta I=1/2$ rule. The domain of validity of this relation is determined.

A review of inclusion of baryons in chiral perturbation theory is given and one-loop corrections to the Gell-Mann-Okubo relation; semileptonic hyperon decays and nonleptonic S and P wave decays are calculated. All corrections are small except the nonleptonic P wave decays and one S wave decay. The corrections to the Lee-Sugawara relation are large as a consequence of the latter.

Some predictions beyond chiral perturbation theory can be made within the soliton model of baryons. F/D ratios are predicted for hyperon magnetic moments, semileptonic decays and nonleptonic S wave decays in this model.

Table of Contents

I. INTRODUCTION.

In this work we study the interface between the standard model that describes leptons and quarks and the observed low-energy phenomena involving leptons, mesons and baryons. The approach we 'll take is to use the standard model to determine which four fermion operators are important at the weak scale ($\mu=M_W$). We then use renormalization group equations to determine the operator structure at low energies ($\mu\approx 1\,GeV$). This is done in Chapter II.

The next problem is to connect this known operator structure to experiment. We do this by using the symmetries of this operator structure and reproducing these symmetry properties in an effective theory involving mesons and baryons. This method is known (for this case) as chiral perturbation theory and is described in Chapter III for a purely mesonic theory. Incorporation of baryons is discussed in Chapter VI. In Chapter IV we use chiral perturbation theory to study some predictions in CP violating phenomena in the $K^0-\bar{K}^0$ system including one-loop non-analytic corrections to the B parameter.

The next Chapter uses the same techniques to examine the validity of a relation between $K\pi\pi$, $K\pi$ and K-vacuum amplitudes that is often used in attempts to explain the $\Delta I=\frac{1}{2}$ rule using lattice QCD Monte Carlo methods.

The last two Chapters deal with processes involving baryons. In Chapter VI we describe the conventional approach to include baryons in the chiral Lagrangian. We rederive some classic current algebra results now, including the leading nonanalytic corrections to estimate their theoretical accuracy.

The last Chapter shows how the soliton model for baryons allows some predictions beyond those of the previous Chapter.

II. THE EFFECTIVE WEAK HAMILTONIAN[f1].

1. At the weak scale.

In the standard six-quark model [1,2] the weak current is given by

$$J_\mu^{(+)}=\frac{g_2}{\sqrt{2}}\left(\bar{u}_L\ \bar{c}_L\ \bar{t}_L\right)\gamma_\mu U\begin{pmatrix}d_L\\ s_L\\ b_L\end{pmatrix}, \tag{2.1}$$

with

$$q_L=\frac{1-\gamma_5}{2}q \tag{2.2}$$

and U a 3×3 unitary matrix that arises from the diagonalization of the quark-mass matrix. Redefining phases of quark fields allows U to be put in the form [2]

$$U=\begin{pmatrix} c_1 & -s_1c_3 & -s_1s_3 \\ s_1c_2 & c_1c_2c_3-s_2s_3e^{i\delta} & c_1c_2s_3+s_2c_3e^{i\delta} \\ s_1s_2 & c_1s_2c_3+c_2s_3e^{i\delta} & c_1s_2s_3-c_2c_3e^{i\delta}\end{pmatrix}. \tag{2.3}$$

In (2.3) $c_i=\cos\theta_i$ and $s_i=\sin\theta_i$. $\theta_{1,2,3}$ are angles in the first quadrant. The CP violating phase δ cannot be removed unless one of the angles is zero.

Weak decays are mediated by the graphs of Fig. (1). We will work here to lowest order in electromagnetic and weak interactions and to leading logarithmic order in heavy masses in strong interactions (QCD). Because the quark current appearing in semileptonic decays is partially

---

[f1] This Chapter follows [3] closely. Inclusion of electromagnetic effects has been published in [5]. The principle of an effective weak theory has been discussed in [6].

conserved by the strong interactions the four fermion operators describing this don't scale. We will, therefore, concentrate on purely hadronic processes in this Chapter.

The effects of one W exchange to leading order in the W mass are reproduced by the effective Hamiltonian (only strangeness changing part) for a subtraction point $\mu=M_W$.[f2]

$$H_{eff}=-\frac{G_F}{2\sqrt{2}}\left[A_c\,(O_c^{(+)}+O_c^{(-)})+A_t\,(O_t^{(+)}+O_t^{(-)})\right]. \tag{2.4}$$

In eq. (2.4)

$$A_c=s_1c_2(c_1c_2c_3-s_2s_3e^{-i\delta}), \tag{2.5a}$$

$$A_t=s_1s_2(c_1s_2c_3-c_2s_3e^{-i\delta}) \tag{2.5b}$$

and

$$O_q^{(\pm)}=\left[(\bar{s}_\alpha u_\alpha)_L(\bar{u}_\beta d_\beta)_L\pm(\bar{s}_\alpha d_\alpha)_L(\bar{u}_\beta u_\beta)_L\right]-\left[u\to q\right]. \tag{2.6}$$

[f2] $(q_\alpha q_\alpha)_L(q_\beta q_\beta)_R$ in eq. (2.6) means $\bar{q}_\alpha\gamma_\mu(1-\gamma_5)q_\alpha\;\bar{q}_\beta\gamma^\mu(1+\gamma^5)q_\beta$; α and β are color indices and are summed over.

2. Between M_W and m_t.

The effective Hamiltonian can be written as

$$H_{eff}=\sum_i C_i(\mu)O_i, \tag{2.7}$$

where the Wilson coefficients $C_i(\mu)$ satisfy the renormalization group equation (in a mass-independent subtraction scheme)

$$\left[\left(\mu\frac{\partial}{\partial\mu}+\beta(g)\frac{\partial}{\partial g}\right)\delta_{ij}-\gamma_{ji}\right]C_j(\mu,g)=0. \tag{2.8}$$

The coefficients γ_{ij} are defined by the relation between bare operators O_j^0 and renormalized operators O_j via

$$O_j^0=Z_{ji}O_i \tag{2.9a}$$

and

$$\gamma_{ij}=(Z^{-1})_{ik}\mu\frac{\partial}{\partial\mu}Z_{kj}. \tag{2.9b}$$

The eigenvectors of γ^T correspond to multiplicatively renormalized operators. At one loop and with six quarks these are precisely the operators $O_q^{(\pm)}$. The penguin diagrams from Fig. (2) don't cause mixing with other operators because of GIM cancellations. In Landau gauge we have from the diagrams like Fig.(3)

$$\gamma_{++}=\frac{g^2}{4\pi^2} \tag{2.10a}$$

$$\gamma_{--}=-\frac{g^2}{2\pi^2}. \tag{2.10b}$$

Solving the renormalization group equation in the standard way gives the effective Hamiltonian at $\mu=m_t$:

$$H_{eff} = -\frac{G_F}{2\sqrt{2}}\left\{\left[\frac{\alpha(M_W)}{\alpha(m_t)}\right]^{2/7}\left(A_c\, O_c^{(+)} + A_t\, O_t^{(+)}\right) + \left[\frac{\alpha(M_W)}{\alpha(m_t)}\right]^{-4/7}\left(A_c\, O_c^{(-)} + A_t\, O_t^{(-)}\right)\right\}. \tag{2.11}$$

$\alpha(\mu)$ here is the running structure constant in the six-quark theory.

3. Below m_t.

We now treat the top quark as heavy and remove it from the theory. The diagram in Fig. (2) now causes mixing because GIM cancellation no longer functions.

Using the QED and QCD equations of motion, Fig. (2) contributes to the mixing of four fermion operators. Operators O_7 and O_8 are introduced via a photon in Fig. (2). For the other operators electromagnetic effects are negligible, since $\alpha_S \gg \alpha_e$.

The operators needed are

$$O_1=(\bar{s}_\alpha d_\alpha)_L(\bar{u}_\beta u_\beta)_L \tag{2.12a}$$

$$O_2=(\bar{s}_\alpha d_\beta)_L(\bar{u}_\beta u_\alpha)_L \ , \tag{2.12b}$$

$$O_3=(\bar{s}_\alpha d_\alpha)_L\Big[(\bar{u}_\beta u_\beta)_L+(\bar{d}_\beta d_\beta)_L+(\bar{s}_\beta s_\beta)_L+(\bar{c}_\beta c_\beta)_L+(\bar{b}_\beta b_\beta)_L\Big], \tag{2.12c}$$

$$O_4=(\bar{s}_\alpha d_\beta)_L\Big[(\bar{u}_\beta u_\alpha)_L+(\bar{d}_\beta d_\alpha)_L+(\bar{s}_\beta s_\alpha)_L+(\bar{c}_\beta c_\alpha)_L+(\bar{b}_\beta b_\alpha)_L\Big], \tag{2.12d}$$

$$O_5=(\bar{s}_\alpha d_\alpha)_L\Big[(\bar{u}_\beta u_\beta)_R+(\bar{d}_\beta d_\beta)_R+(\bar{s}_\beta s_\beta)_R+(\bar{c}_\beta c_\beta)_R+(\bar{b}_\beta b_\beta)_R\Big], \tag{2.12e}$$

$$O_6=(\bar{s}_\alpha d_\beta)_L\Big[(\bar{u}_\beta u_\alpha)_R+(\bar{d}_\beta d_\alpha)_R+(\bar{s}_\beta s_\alpha)_R+(\bar{c}_\beta c_\alpha)_R+(\bar{b}_\beta b_\alpha)_R\Big], \tag{2.12f}$$

$$O_7=\frac{e^2}{g'^2}(\bar{s}_\alpha d_\alpha)_L\Big[(\bar{u}_\beta u_\beta)_L-\tfrac{1}{2}(\bar{d}_\beta d_\beta)_L+(\bar{c}_\beta c_\beta)_L-\tfrac{1}{2}(\bar{s}_\beta s_\beta)_L-\tfrac{1}{2}(\bar{b}_\beta b_\beta)_L\Big], \tag{2.12g}$$

$$O_8=\frac{e^2}{g'^2}(\bar{s}_\alpha d_\beta)_L\Big[(\bar{u}_\beta u_\alpha)_R-\tfrac{1}{2}(\bar{d}_\beta d_\alpha)_R+(\bar{c}_\beta c_\alpha)_R-\tfrac{1}{2}(\bar{s}_\beta s_\alpha)_R-\tfrac{1}{2}(\bar{b}_\beta b_\alpha)_R\Big]. \tag{2.12h}$$

In $O_{7,8}$ we introduced e^2/g'^2 to make all coefficients in the anomalous dimension matrix of the same order in g'^2 [f3].

[f3] A similar situation occurred in Ref. [7].

g' is the running coupling constant for QCD with 5 quarks.

The anomalous dimension matrix is given by

$$\gamma'_{ij}=\frac{g'^2}{8\pi^2}\begin{bmatrix} -1 & 3 & 0 & 0 & 0 & 0 & 8/9 & 0 \\ 3 & -1 & -1/9 & 1/3 & -1/9 & 1/3 & 8/27 & 0 \\ 0 & 0 & -11/9 & 11/3 & -2/9 & 2/3 & 4/27 & 0 \\ 0 & 0 & 22/9 & 2/3 & -5/9 & 5/3 & -20/27 & 0 \\ 0 & 0 & 0 & 0 & 1 & -3 & 4/9 & 0 \\ 0 & 0 & -5/9 & 5/3 & -5/9 & -19/3 & 4/27 & 0 \\ 0 & 0 & 0 & 0 & 0 & 0 & -20/3 & -3 \\ 0 & 0 & 0 & 0 & 0 & 0 & 0 & -47/3 \end{bmatrix} \quad (2.13)$$

We now diagonalize γ^T and run the renormalization group down to $\mu=m_b$ numerically. The values of $C_i(m_t)$ are chosen so that matrix elements of H_{eff} not involving a top quark are continuous across $\mu=m_t$ to lowest order in inverse powers of m_t. At $\mu=m_b$ we introduce a new set of operators $Q_1,\ldots,Q_8$ identical to $O_1,\ldots,O_8$ except that all b quark fields have been removed and in $Q_{7,8}$ g'^2 is replaced by g''^2, the running coupling constant in the four-quark model.

The anomalous dimension matrix for $Q_1,\ldots,Q_8$ is given by

$$\gamma''_{ij}=\frac{g''^2}{8\pi^2}\begin{bmatrix} -1 & 3 & 0 & 0 & 0 & 0 & 8/9 & 0 \\ 3 & -1 & -1/9 & 1/3 & -1/9 & 1/3 & 8/27 & 0 \\ 0 & 0 & -11/9 & 11/3 & -2/9 & 2/3 & 16/27 & 0 \\ 0 & 0 & 23/9 & 1/3 & -4/9 & 4/3 & -16/27 & 0 \\ 0 & 0 & 0 & 0 & 1 & -3 & 8/9 & 0 \\ 0 & 0 & -4/9 & 4/3 & -4/9 & -20/3 & 8/27 & 0 \\ 0 & 0 & 0 & 0 & 0 & 0 & -22/3 & -3 \\ 0 & 0 & 0 & 0 & 0 & 0 & 0 & -47/3 \end{bmatrix} \quad (2.14)$$

Then we run the renormalization group to $\mu=m_c$. At this scale we remove the charm quark and introduce operators $P_1,\ldots,P_6$, P'_7 and P'_8 (with c fields omitted from $Q_1,\ldots,Q_8$ and g''^2 replaced by g'''^2). Now, P_4 is a linear combination of P_1, P_2 and P_3. The anomalous

dimension matrix for the P_i without P_4 is

$$\gamma'''_{ij}=\frac{g'''^2}{8\pi^2}\begin{bmatrix} -1 & 3 & 0 & 0 & 8/9 & 0 \\ 8/3 & -2/3 & 2/9 & -1/9 & 8/27 & 0 \\ -11/3 & 11/3 & 22/9 & -2/9 & -8/27 & 0 \\ 0 & 0 & 0 & 1 & 0 & 0 \\ -1 & 1 & 2/3 & -1/3 & 0 & 0 \\ 0 & 0 & 0 & 0 & -8 & -3 \\ 0 & 0 & 0 & 0 & 0 & -17 \end{bmatrix}. \qquad (2.15)$$

We then run the renormalization group to a scale μ where $\alpha_S(\mu)=1$. Defining P_7, P_8 by $g'''^2/e^2 \times P'_7$, P'_8, the effective Hamiltonian for strangeness changing weak decays can be written as

$$H_{eff}=-\frac{G_F}{\sqrt{2}} s_1 c_1 c_3 \sum_{i=1}^{8}{}' C_i(\mu) P_i, \qquad (2.16)$$

where $\sum_{i=1}^{8}{}'$ means the sum with P_4 omitted. Values for the coefficients C_i using M_W=80 *GeV*, m_t=30 *GeV*, m_b=4.5 *GeV*, m_c=1.5 *GeV*, $\alpha_S(\mu)$=1 and Λ''^2=0.01 *GeV*^{2} and 0.1 *GeV*^{2} are given in Table 1.

4. The $\Delta S=2$ effective Hamiltonian.

This has been derived in [4] using similar methods. The result (which we will need later) is

$$H_{eff}^{\Delta S=2}=-\frac{G_F^2}{16\pi^2}\,(\bar{d}_\alpha s_\alpha)_L(\bar{d}_\beta s_\beta)_L\left[\tilde{\eta}_1 m_c^2+\tilde{\eta}_2 m_t^2+2\tilde{\eta}_3 m_c^2\ln\frac{m_t^2}{m_c^2}\right], \quad (2.17)$$

where $\tilde{\eta}_i$ is given by

$$\tilde{\eta}_1=\eta_1 s_1^2 c_2^2(c_1c_2c_3-s_2s_3e^{-i\delta})^2, \quad (2.18a)$$

$$\tilde{\eta}_2=\eta_2 s_1^2 s_2^2(c_1s_2c_3+c_{2_3}e^{-i\delta})^2, \quad (2.18b)$$

$$\tilde{\eta}_3=\eta_3 s_1^2 s_2 c_2(c_1c_2c_3-s_2s_3e^{-i\delta})(c_1s_2c_3+c_2s_3e^{-i\delta}). \quad (2.18c)$$

For the same parameters as used in the previous section the coefficients η_1, η_2, η_3 are listed in Table 2.

III. CHIRAL PERTURBATION THEORY.

1. The Lagrangian to lowest order.

The previous chapters contained quarks but the observed strongly interacting particles are mesons and baryons. Since at present no fundamental derivation of the structure of baryons and mesons from QCD exists, we will use the approximate symmetries present in the QCD Lagrangian to make predictions about the low-energy states. The symmetry we will use is chiral $SU(3)_L \times SU(3)_R \times U(1)_V$ ($U(1)_A$ is broken by anomalies). The $U(1)_V$ plays no role in the rest of this work except to conserve baryon number.

Chiral symmetry is broken by vacuum expectation values [f1]

$$<\bar{q}^i_R q_{Lj}> = v\Sigma^i_j \quad . \tag{3.1}$$

v is a scalar with the dimension of mass. i,j are flavor indices. The 3×3 matrix Σ describes the different vacua connected by $SU(3)_L \times SU(3)_R$ transformations. Under an $SU(3)_L \times SU(3)_R$ transformation

$$q'_{Li} = L^i_j q_{Lj} \tag{3.2a}$$

$$q'_{Ri} = R^i_j q_{Rj}. \tag{3.2b}$$

From (3.1) we then see that

$$\Sigma' = L\Sigma R^\dagger. \tag{3.3}$$

[f1] For a review of chiral symmetry, see [8].

Since Σ describes the orientation of the vacuum it should contain the Goldstone boson degrees of freedom. It is parameterized via

$$\Sigma=\exp\frac{2i}{f}M \tag{3.4}$$

and

$$M=\begin{pmatrix} \frac{\pi^0}{\sqrt{2}}+\frac{\eta}{\sqrt{6}} & \pi^+ & K^+ \\ \pi^- & -\frac{\pi^0}{\sqrt{2}}+\frac{\eta}{\sqrt{6}} & K^0 \\ K^- & \bar{K}^0 & -\left(\frac{2}{3}\right)^{1/2}\eta \end{pmatrix}. \tag{3.5}$$

We now use Σ to construct a Lagrangian describing the Goldstone bosons; that is, $SU(3)_L\times SU(3)_R$ symmetric [f2].

$$L_0=\frac{f^2}{8}tr\,\partial_\mu\Sigma\partial^\mu\Sigma^\dagger \tag{3.6a}$$

to lowest order in derivatives. Terms with more derivatives are suppressed by $\frac{q^2}{\Lambda_c^2}$. q^2 is a typical mass or momentum squared and Λ_c is the chiral symmetry-breaking scale. Λ_c is expected to be of order $4\pi f_\pi$ [10].

Chiral symmetry is also broken by the "bare" quark masses. We also expand in this breaking (an expansion in $\frac{m_q}{\Lambda_c}$). The first term in this expansion is

$$L_{m1}=v\ tr(m\Sigma+m\Sigma^\dagger) \tag{3.6b}$$

[f2] Different nonlinear realizations of a symmetry are equivalent in the loop expansion [9].

with m the quark mass matrix.

$$m=\begin{pmatrix} m_u & 0 & 0 \\ 0 & m_d & 0 \\ 0 & 0 & m_s \end{pmatrix}. \tag{3.7}$$

f is measured via the pion decay constant f_π and v via the meson masses. Expanding Σ to quadratic order and identifying terms in the Lagrangian gives

$$v=\frac{f^2m_K^2}{4(m_d+m_s)}=\frac{f^2m_\pi^2}{8m_d}=\frac{3}{4}f^2\frac{m_\eta^2}{4m_s+2m_d}. \tag{3.8}$$

In (3.8) we have set $m_u=m_d$. Throughout the rest of this work we will keep this and hence have isospin as a good symmetry.

From (3.8) we see that one power of a quark mass is equivalent to two powers of a Goldstone boson mass or two derivatives in our expansion of the chiral Lagrangian.

To determine f we derive the left-handed current from (3.6)

$$j_\mu^{La}=-\frac{if^2}{4}trT^a\partial_\mu\Sigma\Sigma^\dagger \tag{3.9}$$

and in π^+ decay we define f_π to be

$$<0|j_\mu^{L1+i2}|\pi^+>=-\frac{i}{2}f_\pi p_{\pi\mu} \tag{3.10}$$

where

$$T^{1+i2}=\begin{pmatrix} 0 & 0 & 0 \\ 1 & 0 & 0 \\ 0 & 0 & 0 \end{pmatrix}. \tag{3.11}$$

Expanding (3.10) then gives

$$f=f_\pi. \tag{3.12}$$

2. Weak nonleptonic decays to leading order.

The strangeness changing effective Hamiltonian contains octet and 27 operators. The lowest-dimension operator constructed using Σ that transforms as $(8_L,1_R)$ under $SU(3)_L\times SU(3)_R$ is

$$O^{(8)}= a\ tr\,T_L\partial_\mu\Sigma\partial^\mu\Sigma^\dagger + b\ tr\,(mT_L\Sigma+m\Sigma^\dagger T_L) \tag{3.13}$$

and the operator that transforms as $(27_L,1_R)$ is

$$O^{(27)}= c\ T^{ij}_{kl}(\Sigma\partial_\mu\Sigma^\dagger)^k_i(\Sigma\partial^\mu\Sigma^\dagger)^l_j. \tag{3.14}$$

For $\Delta S=1$ nonleptonic decays we have

$$T_L=\begin{pmatrix}0&0&0\\0&0&0\\0&1&0\end{pmatrix} \tag{3.15}$$

and the only nonzero elements of T^{kl}_{ij} are

$$T^{13}_{12} = T^{31}_{12} = T^{13}_{21} = T^{31}_{21} = -T^{23}_{22} = -T^{32}_{22} = \tfrac{1}{2}. \tag{3.16}$$

The term proportional to b doesn't contribute to on-shell processes because it is a total derivative for T_L given in (3.15) if $m_d\neq m_s$ [f3].

The variation of the Lagrangian (3.6) under an infinitesimal left-handed transformation $1-iT_L$ is given by

$$\delta L=-itr\,(mT_L\Sigma-m\Sigma^\dagger T_L) \tag{3.19}$$

and from Noether's theorem

$$\delta L=\partial_\mu j^\mu_L. \tag{3.20}$$

[f3] I thank H. Sonoda for this observation.

Expanding (3.13), (3.19) and (3.20) in powers of M then shows that the 2nd term in (3.13) can be written as a total divergence.

The effective Hamiltonian also contains parts that transform as $(8_L,8_R)$. The lowest-dimension operator that transforms this way is

$$tr\, T_L \Sigma T_R \Sigma^\dagger. \tag{3.21}$$

T_L is given by (3.15) and T_R is

$$T_R = \begin{pmatrix} 2 & 0 & 0 \\ 0 & -1 & 0 \\ 0 & 0 & -1 \end{pmatrix}. \tag{3.22}$$

Since (3.21) contains no derivatives its matrix elements are expected to be $O\left(\frac{4\pi f_\pi{}^2}{m_K^2}\right)(\approx 10)$ larger than those of (3.13) and (3.14). This is why the electromagnetic effects, corresponding to operators P_7, P_8 in Chapter II, can contribute significantly to ε'/ε[f4].

Apart from order of magnitude estimates between matrix elements of operators transforming in different representations under $SU(3)_L \times SU(3)_R$, more accurate relations can be established between matrix elements of operators in the same $SU(3)_L \times SU(3)_R$ representation. In this case the unknown numerical constant in front of the operators doesn't matter.

As an example we rederive a relation between a $K \to 2\pi$ and a $K \to 3\pi$ matrix element[11]. We start with expanding $O^{(8)}$ (for on-shell matrix elements and $m_d = m_u = 0$).

$$O^{(8)} = \frac{4a}{f^2}(\partial_\mu M \partial^\mu M)\frac{3}{2} + \cdots$$

[f4] This parameter is defined in the next Chapter.

$$= -\frac{4a}{\sqrt{2}f^2}\partial_\mu K^0 \partial^\mu \pi^0 + \cdots \tag{3.23}$$

$<\pi^0\pi^0|O^{(8)}|K^0>$ gets contributions from Fig.(4). A dark square in Figs.(4,5) is an insertion of $O^{(8)}$. The result is

$$<\pi^0\pi^0|O^{(8)}|K^0> = \frac{4ia}{f^3}m_K^2. \tag{3.24}$$

$<\pi^0\pi^0\pi^0|O^{(8)}|K^0>$ gets contributions from the diagrams in Figs.(5). A dark circle is an insertion of the lowest-order strong interaction Lagrangian (3.6). The contributions from Figs.(5b.c) vanish and Fig.(5a) gives

$$<\pi^0(k_1)\pi^0(k_2)\pi^0(k_3)|O^{(8)}|K^0(k)> = \frac{4\sqrt{2}a}{3f^4}(k\cdot k_1 + k_1\cdot k_2)$$

$$+ \textit{cycl. perm. in } (1,2,3)$$

$$= \frac{2\sqrt{2}a}{f^4}m_K^2. \tag{3.25}$$

Notice that this satisfies the classic current algebra relation [11,13].

3. Beyond lowest order.

The chiral Lagrangian method can be used to go beyond lowest order[12,13]. This is also possible within the framework of current algebra but the calculations are less transparent [14-17].

Since we include all terms up to a given order in $\frac{q^2}{\Lambda_c^2}$ in the Lagrangian and the operators, we can absorb all infinities into redefinitions of the bare parameters[12]. In this way the parameters become renormalization point dependent in such a way that physical quantities do not depend on it.

Higher-order terms coming directly from higher-dimension operators will always depend analytically on $\frac{q^2}{\Lambda_c^2}$ and $\frac{m^2}{\Lambda_c^2}$. The nonanalytic dependence on Goldstone boson masses and momenta has to come from diagrams with loops and insertions of lower-dimension operators. These parts of higher-order terms can thus be extracted uniquely from loop diagrams involving vertices from the lower dimension operators[12,15].

As an example of this we will calculate in this section the leading nonanalytic correction for $m_{K,\pi,\eta}$ and f_π. We will only encounter logarithmic nonanalyticities in this section.

Formulas in the remainder of this chapter are correct in two cases, $m_u=m_d\approx m_s$ and $m_u=m_d=0$, $m_s\neq 0$. In this case we don't have to distinguish between logarithms with different arguments. All logarithms will be written as $\log\frac{m_K^2}{\mu^2}$ where μ is the renormalization point.

In all these cases the logarithm would dominate the next order correction if it was large (which would be the case if the meson masses were really small). In practice for logarithms involving a kaon mass this

logarithm is about 4, so there is no reason to expect this piece to dominate the correction. The attitude we take is that if the logarithmic part is small we believe the total correction to be small and we will use the lowest-order result with confidence. If the logarithmic part is large, we probably also have a large correction from the higher-order terms and we will not use the lowest-order result to make predictions.

The field renormalization[f5] comes from the diagram in Fig.(6). Only an insertion of (3.6a) with the derivatives acting on the outside legs contributes to Z.

For Z_K the relevant terms in L_0 are

$$L_0=-\frac{1}{3f^2}\partial_\mu K^0\partial^\mu\bar{K}^0(\pi^+\pi^- + \frac{1}{2}\pi^0\pi^0 + 2K^0\bar{K}^0 + \frac{3}{2}\eta\eta) \tag{3.26}$$

and the loop integral (see App. B) is

$$\int\frac{d^4p}{(2\pi)^4}\frac{i}{p^2-m^2}=\frac{m^2}{16\pi^2}\log\frac{m^2}{\mu^2}. \tag{3.27}$$

This leads to

$$\begin{aligned} Z_K&=1+\frac{1}{16\pi^2f^2}\left[\frac{1}{2}m_\pi^2\log\frac{m_\pi^2}{\mu^2} + m_K^2\log\frac{m_K^2}{\mu^2} + \frac{1}{2}m_\eta^2\log\frac{m_\eta^2}{\mu^2}\right] \\ &=1+\frac{1}{16\pi^2f^2}\left[\frac{1}{3}m_\pi^2 + \frac{5}{3}m_K^2\right]\log\frac{m_K^2}{\mu^2}. \end{aligned} \tag{3.28}$$

Similarly, the relevant term in L_0 for Z_π is

$$L_0=-\frac{1}{6f^2}\partial_\mu\pi^0\partial^\mu\pi^0(4\pi^+\pi^- + K^+K^- + K^0\bar{K}^0) \tag{3.29}$$

leading to

[f5] For a definition of Z see Appendix A.

$$Z_\pi = 1 + \frac{1}{16\pi^2 f^2}\left[\frac{4}{3}m_\pi^2 + \frac{2}{3}m_K^2\right]\log\frac{m_K^2}{\mu^2}. \tag{3.30}$$

In the same way we derive

$$L_0 = -\frac{1}{2}f^2\partial_\mu\eta\partial^\mu\eta(K^+K^- + K^0\bar{K}^0) \tag{3.31}$$

and

$$Z_\eta = 1 + \frac{1}{16\pi^2 f^2}2m_K^2\log\frac{m_K^2}{\mu^2}. \tag{3.32}$$

In all these formulas we used the Gell-Mann-Okubo relation[28]

$$m_\eta^2 = \frac{4}{3}m_K^2 - \frac{1}{3}m_\pi^2. \tag{3.33}$$

This follows from (3.8).

Notice that for $m_u = m_d = m_s$ $SU(3)_V$ symmetry is restored in the Z's.

At this level the relations (3.12) and (3.8) are no longer valid. Evaluating the correction to the matrix element in (3.10) due to field renormalization and from the diagram in Fig.(7) we get (the relevant integral here is also (3.27))

$$<0|j_\mu^{L1+i2}|\pi^+> = -\frac{i}{2}p_{\pi\mu}f\left[1 + \frac{1}{16\pi^2 f^2}(-m_K^2 - 2m_\pi^2)\log\frac{m_K^2}{\mu^2}\right]. \tag{3.34}$$

Using the definition (3.10) of f_π this means

$$f = f_\pi\left[1 + \frac{1}{16\pi^2 f_\pi^2}(m_K^2 + 2m_\pi^2)\log\frac{m_K^2}{\mu^2}\right]. \tag{3.35}$$

The equations (3.28-35) depend on the renormalization scale μ, but this dependence cancels against the μ dependence of the coefficients of the higher-dimension operators so that physical quantities do not depend on it.

To calculate the correction to (3.8) we have to evaluate the diagram in Fig.(6) with the circle an insertion (3.6) with no derivatives acting on the outside legs.

Using App. A to evaluate the mass corrections and using (3.8) in the correction terms we get[f6]

$$m_K^2=\frac{4v}{f^2}(m_d+m_s)+\frac{1}{16\pi^2f^2}\left[-\frac{2}{9}m_\pi^2m_K^2+\frac{8}{9}m_K^4\right]\log\frac{m_K^2}{\mu^2}, \tag{3.36a}$$

$$m_\pi^2=\frac{8v}{f^2}m_d+\frac{1}{16\pi^2f^2}\left[\frac{4}{9}m_\pi^4+\frac{2}{9}m_\pi^2m_K^2\right]\log\frac{m_K^2}{\mu^2}, \tag{3.36b}$$

$$m_\eta^2=\frac{8v}{3f^2}(2m_s+m_d)+\frac{1}{16\pi^2f^2}\left[-\frac{34}{27}m_\pi^4+\frac{44}{27}m_\pi^2m_K^2+\frac{8}{27}m_K^4\right]\log\frac{m_K^2}{\mu^2}. \tag{3.36c}$$

Notice that here we also have $SU(3)_V$ restored when all the quark masses are equal.

Using this, the Gell-Mann-Okubo relation becomes

$$\frac{3}{4}m_\eta^2+\frac{1}{4}m_\pi^2-m_K^2=\frac{1}{16\pi^2f^2}\left[-\frac{5}{6}m_\pi^4+\frac{3}{2}m_\pi^2m_K^2-\frac{2}{3}m_K^4\right]\log\frac{m_K^2}{\mu^2}. \tag{3.37}$$

The corrections calculated in this section are all small, around 15% or smaller, indicating that chiral perturbation theory is valid in all these cases.

[f6] This disagrees with the results of Ref. [16]. The numerical result however agrees since we differ only in the (small) m_π^2 dependence.

IV. CHIRAL PERTURBATION THEORY AND $K^0-\bar{K}^0$ MIXING.

1. Parameters of CP violation.

An overview of the phenomenology has been given in [19] and references therein. All CP violation observed so far has been in the neutral kaon system. Searches for an electric dipole moment of the neutron and CP violation in charged kaon decays have only produced upper bounds.

We describe the neutral kaon system by a two-state wave function

$$\psi=\begin{pmatrix}a\\b\end{pmatrix}\equiv a\,|K^0>+b\,|\bar{K}^0> \tag{4.1}$$

and a Hamiltonian

$$H=M-i\Gamma\ . \tag{4.2}$$

In (4.2) M and Γ are Hermitian 2×2 matrices.

The mass eigenstates of this system are

$$K_{S,L}=\frac{1}{(2(1+|\varepsilon|^2))^{\frac{1}{2}}}\left[(1+\varepsilon)K^0\pm(1-\varepsilon)\bar{K}^0\right]. \tag{4.3}$$

ε describes the deviation of the mass eigenstates from the CP eigenstates $K^0\pm\bar{K}^0$.

Defining m_S, m_L and Γ_S, Γ_L to be the eigenvalues of M and Γ we have that

$$\varepsilon=\frac{i\mathrm{Im}\Gamma_{12}-\mathrm{Im}M_{12}}{(\Gamma_S-\Gamma_L)/2+i(m_S-m_L)}\ . \tag{4.4}$$

In the phase convention where

$$A_0=<(\pi\pi)_{I=0}|H_{weak}|K^0> \tag{4.5}$$

is real we have that

$$\mathrm{Im}\Gamma_{12} \ll \mathrm{Im}M_{12} \tag{4.6}$$

assuming that Γ_{12} comes mainly from the lightest intermediate state (the $\pi\pi$ intermediate state).

Using then

$$m_S - m_L = 2\mathrm{Re}M_{12} \tag{4.7}$$

and the experimental result

$$m_S - m_L \approx -\frac{1}{2}(\Gamma_S - \Gamma_L) \tag{4.8}$$

ε reduces to

$$\varepsilon = \frac{1}{\sqrt{2}} \frac{\mathrm{Im}M_{12}}{m_S - m_L} e^{i\frac{\pi}{4}}. \tag{4.9}$$

In (4.9) we used (4.7) instead of the short-distance prediction for $\mathrm{Re}M_{12}$ because the long-distance contribution to $\mathrm{Re}M_{12}$ is probably not small while a small improvement on the experimental limit on $\frac{\varepsilon'}{\varepsilon}$ (see further) makes the $\pi\pi$ intermediate-state contribution to $\mathrm{Im}M_{12}$ small so that probably a short-distance evaluation of $\mathrm{Im}M_{12}$ is sufficient.

We define

$$A_2 = <(\pi\pi)_{I=2}|H_{weak}|K^0>. \tag{4.10}$$

Using this we can define ε'

$$\varepsilon' = \frac{i}{\sqrt{2}} e^{i(\delta_2 - \delta_0)} \mathrm{Im}\left[\frac{A_2}{A_0}\right]. \tag{4.11}$$

In (4.11) δ_0, δ_2 are the phase shifts in isospin 2, 0 $\pi\pi$ scattering.

Roughly speaking, ε describes CP violation in $\Delta S=2$ transitions and ε' in $\Delta S=1$ transitions.

Experimentally ε, $\frac{\varepsilon'}{\varepsilon}$ and $\frac{A_2}{A_0}$ are small. To leading order in these quantities we have[20]

$$\eta_{+-}=\frac{<\pi^+\pi^-|H_{weak}|K_L>}{<\pi^+\pi^-|H_{weak}|K_S>}\approx\varepsilon+\varepsilon' \tag{4.12}$$

and

$$\eta_{00}=\frac{<\pi^0\pi^0|H_{weak}|K_L>}{<\pi^0\pi^0|H_{weak}|K_S>}\approx\varepsilon-2\varepsilon'. \tag{4.13}$$

Both η_{+-} and η_{00} are measured to be nonzero and are the only place where CP violation has been observed so far.

Experimentally we have [19]

$$|\varepsilon|\approx 2.3\ 10^{-3} \tag{4.14}$$

$$\frac{\varepsilon'}{\varepsilon}\approx(-4.6\pm5.3\pm2.4)\times10^{-3}. \tag{4.15}$$

In the minimal standard model this observed CP violation has to come from the phase δ in (2.3). The stringent limit on the electric dipole moment of the neutron[21] makes the θ parameter in the QCD Lagrangian far too small to account for the CP violation in the kaon system.

From (4.9) and (2.17) we then get

$$\varepsilon\approx-\frac{s_1^2BG_F^2f_\pi m_K^2m_c^2s_2s_3s_\delta}{16\sqrt{2}\pi^2(m_S-m_L)}\left[-\eta_1+\eta_3\log\frac{m_t^2}{m_c^2}+\eta_2\frac{m_t^2}{m_c^2}(s_2^2+s_2s_3c_\delta)\right]e^{i\frac{\pi}{4}}. \tag{4.16}$$

The dimensionless parameter B is defined as

$$<\bar{K}^0|O^{(27)}|K^0>=Bf_\pi m_K^3 \tag{4.17}$$

where

$$O^{(27)}=(\bar{s}_\alpha d_\alpha)_L(\bar{s}_\beta d_\beta)_L. \tag{4.18}$$

The prediction for $\frac{\varepsilon'}{\varepsilon}$ is (using the experimental value of ε)

$$\left|\frac{\varepsilon'}{\varepsilon}\right| = \tag{4.19}$$

$$\left| 6c_2s_3s_\delta \frac{<(\pi\pi)_{I=0}|\sum_{i=1}^{8}{}'\tilde{C}_i(\mu)P_i|K^0>}{0.1\,GeV^3} \right.$$

$$\left. - 120c_2s_2s_3s_\delta \frac{<(\pi\pi)_{I=2}|\tilde{C}_7(\mu)P_7+\tilde{C}_8(\mu)P_8|K^0>}{0.1\,GeV^3} \right|$$

where the dependence on the mixing angles has been made explicit via

$$\mathrm{Im}C_i(\mu)=\tilde{C}_i(\mu)\frac{c_2s_2s_\delta}{c_1c_3} \tag{4.20}$$

and $\tilde{C}_7$, $\tilde{C}_8$ contain α_{em}.

The mixing angles are constrained via data from β decays, hyperon decays and B meson lifetime and branching ratios experiments [19].

$$s_1=0.22, \tag{4.21}$$

$$s_2^2+s_3^2+2s_2s_3c_\delta \approx 3\times10^{-3}\left(\frac{10^{-12}sec}{\tau_B}\right), \tag{4.22}$$

$$s_3^2 \leq 1 \times 10^{-3} \left(\frac{10^{-12} sec}{\tau_B} \right). \tag{4.23}$$

2. B parameter to lowest order.

This analysis was first done in [22].

The operator (4.17) and the $\Delta I=\frac{3}{2}$ part of the $\Delta S=1$ effective Hamiltonian both transform as $(27_L,1_R)$ under chiral symmetry. The $\Delta S=2$ operator corresponds to (3.14) with the only nonzero element of T

$$T_{22}^{33}=1 \tag{4.24}$$

while the $\Delta I=3/2$ part has the nonzero elements given in (3.16).

Since these are both $(27_L,1_R)$ operators, chiral perturbation theory relates matrix elements of these two operators. The coefficient c in (3.14) is the same in both cases.

Expanding (3.14) for two matrix elements gives

$$<\bar{K}^0|O^{(27)}|K^0>=-\frac{8cm_K^2}{f^2} \tag{4.25}$$

and

$$<\pi^0\pi^+|O^{(27)}|K^+>=-\frac{12icm_K^2}{\sqrt{2}f^3}. \tag{4.26}$$

From (4.17) we then get that

$$B=-\frac{8c}{f^3}m_K. \tag{4.27}$$

We picked the decay in (4.26) because it is pure $\Delta I=3/2$. Extracting the $\Delta I=3/2$ part from (2.17) leads to

$$H_{eff}^{\Delta I=3/2}=-\frac{G_F}{2\sqrt{2}}s_1c_1c_3C\,O^{(27)} \tag{4.28}$$

with

$$C \approx 0.4. \tag{4.29}$$

The invariant matrix element for $K^+ \to \pi^0 \pi^+$ decay is

$$M(K^+ \to \pi^+ \pi^0) = -\frac{3iG_F}{8} B s_1 c_1 c_3 C m_K^3. \tag{4.30}$$

Using the measured value of this decay width B is determined to be

$$|B| \approx 0.4. \tag{4.31}$$

This procedure doesn't determine the sign of B because only its square enters into the decay width.

3. The B parameter to one loop.

The results of this section were published in [23]. This section is concerned only with physical matrix elements and for these setting $m_u=m_d=0$ is a good approximation. We then redo the analysis of the previous section but we calculate the matrix elements (4.25) and (4.26) to one loop order in chiral perturbation theory.

The correction to $<\pi^0\pi^+|O^{(27)}|K^+>$ is small, indicating that chiral perturbation theory is valid. Unfortunately, the correction to $<\bar{K}^0|O^{(27)}|K^0>$ is very large, indicating that chiral perturbation theory is not valid for evaluations of this matrix element.

This means that the value of B derived in the previous section is unreliable and should not be used to constrain significantly the parameters of the standard six-quark model[19].

(4.25) gets corrections from field renormalization and the diagrams in Fig.(8). The black square is an insertion of $O^{(27)}$ and the dot is an insertion of the strong interaction (3.6).

Fig.(8a) contributes

$$\frac{26}{3}\frac{8cm_K^2}{f^2}\frac{m_K^2}{16\pi^2f^2}, \tag{4.32}$$

and Fig.(8b) contributes

$$\frac{14}{3}\frac{8cm_K^2}{f^2}\frac{m_K^2}{16\pi^2f^2} \tag{4.33}$$

resulting in a matrix element

$$<\bar{K}^0|O^{(27)}|K^0>=-\frac{8cm_K^2}{f^2}\left[1+\frac{1}{16\pi^2f^2}\frac{-35}{3}\log\frac{m_K^2}{\mu^2}\right]. \tag{4.34}$$

The correction term here is as large as the leading term for $\mu \approx 1\,GeV$, $m_K \approx 500\,MeV$ and $f \approx 130\,MeV$.

Similarly, (4.26) gets corrections from the diagrams in Fig.(9) and field renormalization. The diagram in Fig.(9)(a,b,c,d) contributes

$$-\frac{12icm_K^2}{\sqrt{2}f^3}\left(-\frac{17}{3},\ 1,\ -\frac{7}{9},\ \frac{22}{9}\right) \tag{4.35}$$

so that the total matrix element becomes

$$<\pi^+\pi^0|\,O^{(27)}|\,K^0>=-\frac{12icm_K^2}{\sqrt{2}f^3}\left[1-\frac{3}{2}\frac{m_K^2}{16\pi^2f^2}\log\frac{m_K^2}{\mu^2}\right]. \tag{4.36}$$

Including in this the relation between f and f_π the matrix elements become

$$<\bar{K}^0|\,O^{(27)}|\,K^0>=-\frac{8cm_K^2}{f_\pi^2}\left[1-\frac{41}{3}m_K\frac{sup2}{16\pi^2f_\pi^2}\log\frac{m_K^2}{\mu^2}\right], \tag{4.37}$$

$$<\pi^+\pi^0|\,O^{(27)}|\,K^+>=-\frac{12icm_K^2}{\sqrt{2}f_\pi^3}\left[1-\frac{9}{2}\frac{m_K^2}{16\pi^2f_\pi^2}\log\frac{m_K^2}{\mu^2}\right]. \tag{4.38}$$

The corrected value of B can then be obtained from

$$M(K^+\to\pi^+\pi^0)=-\frac{3iG_F}{8}B\,s_1c_1c_3C\,m_K^3\left[1+\frac{55}{6}\frac{m_K^2}{16\pi^2f_\pi^2}\log\frac{m_K^2}{\mu^2}\right]. \tag{4.39}$$

The size of the correction in (4.39) indicates that this formula should not be used to determine a value for B.

V. CHIRAL PERTURBATION THEORY AND THE $\Delta I=\frac{1}{2}$ RULE.

1. Introduction.

The enhancement of the $\Delta I = \frac{1}{2}$ amplitude in hadronic weak decays is a longstanding puzzle. Including large logarithms using perturbative QCD and the renormalization group gives an enhancement of the octet (which is pure $\Delta I = \frac{1}{2}$) part of the effective Hamiltonian compared to the 27 part (which contains $\Delta I = \frac{3}{2}$) [3,24]. However, a significant enhancement in the matrix elements of the four-quark operators is still needed to explain the experimental enhancement.

An attempt has been made within chiral perturbation theory to explain this extra enhancement using the renormalization group. It is, however, only qualitatively useful[18].

One approach is direct calculation of the matrix elements using lattice Monte Carlo methods. Attempts to do this are in progress [25]. In the mesonic sector one needs to calculate matrix elements like $<\pi^0\pi^0|\,O^{(8),(27)}\,|K^0>$ with $O^{(8),(27)}$ a four-quark operator. $O^{(8)}$ and $O^{(27)}$ are defined in [24]. However, it is easier, using present Monte Carlo techniques, to measure $<\pi|\,O^{(8),(27)}\,|K>$ and $<o|\,O^{(8)}\,|K>$ with $<o|$ the vacuum. Chiral perturbation provides a relation between these matrix elements and $<\pi\pi|\,O^{(8),(27)}\,|K>$.

In the next two sections we study this relation further and in the last section we describe a method to test how close to the chiral limit a given lattice calculation is.

2. The lowest order relation.

In [26] a relation between $K\pi\pi$ matrix elements and some matrix elements involving a lower number of mesons was derived. In this section we rederive this relation in such a way that inclusion of the one-loop results is easy to do.

The weak effective Hamiltonian to lowest order in momenta and quark masses for $\Delta S = 1$ decays is given by $O^{(8)}$ and $O^{(27)}$. $O^{(8)}$ transforms like $(8_L, 1_R)$ and $O^{(27)}$ like $(27_L, 1_R)$ under $SU(3)_L \times SU(3)_R$

$$O^{(8)} = a\, tr\, A\partial_\mu\Sigma\partial^\mu\Sigma^\dagger + b\, tr\,(m A\Sigma + A m\Sigma^\dagger) \tag{5.1}$$

$$O^{(27)} = c\, T^{ij}_{kl}(\Sigma\partial_\mu\Sigma^\dagger)_i{}^k(\Sigma\partial_\mu\Sigma^\dagger)_j{}^l\,, \tag{5.2}$$

where

$$A = \begin{pmatrix} 0 & 0 & 0 \\ 0 & 0 & 0 \\ 0 & 1 & 0 \end{pmatrix}, \tag{5.3}$$

and the only nonzero elements of T are

$$T^{13}_{12} = T^{31}_{12} = T^{13}_{21} = T^{31}_{21} = -T^{23}_{22} = -T^{32}_{22} = \tfrac{1}{2}\,. \tag{5.4}$$

The coefficients a, b, c are constants independent of the meson masses. The second term in (5.1) is the divergence of a left-handed current for $m_d \neq m_s$ and doesn't contribute to physical, on-shell, matrix elements (see Chapter III).

The $<\pi\pi|\,O^{(8)}, O^{(27)}|K^0>$ matrix elements are needed for the physical value of the meson masses and for these setting $m_u = m_d = 0$ is a good

approximation. Expanding (5.1) and (5.2) to lowest order gives

$$<\pi^0\pi^0|\,O^{(8)}\,|K^0> = \frac{4ia}{f^3}\,m_K^2 \tag{5.5}$$

$$<\pi^0\pi^0|\,O^{(27)}\,|K^0> = \frac{8ic}{f^3}\,m_K^2\,. \tag{5.6}$$

And having $\Delta I = \frac{1}{2}$ enhancement corresponds to having a large ratio

$$\frac{<\pi^0\pi^0|\,O^{(8)}\,|K^0>}{<\pi^0\pi^0|\,O^{(27)}\,|K^0>} = \frac{a}{2c}\,. \tag{5.7}$$

The $<\pi^0|\,O^{(8),O^{(27)}}\,|K^0>$ and $<o\,|\,0\,|K^0>$ matrix elements don't conserve momentum and get contributions from the second term in (5.1). Since the coefficients a, b and c are independent of the meson masses, we can calculate every matrix element with different masses. Here we have $m_u = m_d \neq 0$ because in lattice calculations all meson masses are nonzero. In lowest order, expanding (5.1) and (5.2) results in

$$<\pi^0|\,O^{(8)}\,|K^0> = \frac{-2\sqrt{2}\,a}{f^2}\,m'_K m'_\pi + \frac{\sqrt{2}}{f^2}(m'_s + m'_d) \tag{5.8}$$

$$<\pi^0|\,O^{(27)}\,|K^0> = \frac{-4\sqrt{2}\,c}{f^2}\,m'''_K m'''_\pi \tag{5.9}$$

$$<o\,|\,O^{(8)}\,|K^0> = \frac{2ib}{f}\,(m''_s - m''_d)\,. \tag{5.10}$$

To obtain $\frac{a}{c}$ we need only values for three independent matrix elements, so measuring these on the lattice is sufficient.

The $\Delta I = \frac{1}{2}$ enhancement in meson decays (5.7) can thus also be measured via

$$\frac{<\pi^0|\,O^{(8)}\,|K^0>}{<\pi^0|\,O^{(27)}\,|K^0>} = y\,\frac{<\pi^0|\,O^{(8)}\,|K^0> + x<o\,|\,O^{(8)}\,|K^0>}{<\pi^0|\,O^{(27)}\,|K^0>} \tag{5.11}$$

with

$$x = \frac{i}{\sqrt{2}f} \frac{m'_s + m'_d}{m''_s - m''_d} = \frac{i}{\sqrt{2}f} \frac{m'^2_K}{m''^2_K - m''^2_\pi} \tag{5.12}$$

$$y = \frac{m'''_K m'''_\pi}{m'_K m'_\pi} \ . \tag{5.13}$$

This agrees with the result obtained in [26]. We have used eq. (3.8) to obtain the second relation in (5.12).

3. The relation to one loop.

In this section we calculate the matrix elements of the previous section to one loop and use this to determine the range of validity of (5.11). The results of this and the next section have been published in [27].

Corrections to the matrix elements (5.5) and (5.6) come from the diagrams in Fig. (10) and from field renormalization of the meson fields. A dot is an insertion of the strong interaction Lagrangian (3.6) and a square is an insertion of $O^{(8)}$, resp. $O^{(27)}$. Adding the different contributions gives

$$<\pi^0\pi^0|O^{(8)}|K^0> = \frac{4\alpha i}{f^3} m_K^2\{1 - \frac{97}{27}\frac{m_K^2}{16\pi^2 f^2}\ln\frac{m_K^2}{\mu^2}\}, \qquad (5.14)$$

and using isospin and the result for $<\pi^0\pi^+|O^{(27)}|K^+>$ calculated in the previous chapter we have

$$<\pi^0\pi^0|O^{(27)}|K^0> = \frac{8ic}{f^3} m_K^2\{1 - \frac{3}{2}\frac{m_K^2}{16\pi^2 f^2}\ln\frac{m_K^2}{\mu^2}\}, \qquad (5.15)$$

so that (5.7) becomes

$$\frac{<\pi^0\pi^0|O^{(8)}|K^0>}{<\pi^0\pi^0|O^{(27)}|K^0>} = \frac{a}{2c}\{1 - \frac{113}{54}\frac{m_K^2}{16\pi^2 f^2}\ln\frac{m_K^2}{\mu^2}\}. \qquad (5.16)$$

μ in (5.14), (5.15) and (5.16) is the subtraction point. The subtraction point dependence of amplitudes is canceled by the subtraction point dependence of the contributions of operators that are higher order in derivatives and quark masses [12,15]. That contribution is not enhanced by a "large" logarithm and is hence less important. For $f \approx 135\,MeV$; $m_K \approx 494\,MeV$ and $\mu \approx 1\,GeV$ the correction in (5.14) and (5.15) is of 0(40%) or less, indicating that chiral perturbation theory is valid for these matrix elements. The correction is about 25% in (5.16). So the

correction to the l.h.s. of (5.12) is small.

Corrections to (5.10) come from the diagram in Fig. (11) and field renormalization and gives

$$<o\,|\,0^{(8)}\,|\,K^0> = \frac{2ib}{f}(m''_s - m''_d)\{1 - \frac{1}{16\pi^2 f^2}$$
$$[\frac{3}{4}m''^2_\pi \ln\frac{m''^2_\pi}{\mu^2} + \frac{3}{2}m''^2_K \ln\frac{m''^2_K}{\mu^2} + \frac{1}{12}m''^2_\eta \ln\frac{m''^2_\eta}{\mu^2}]\}$$
$$+ \frac{ia}{16\pi^2 f^2}\{-6m''^4_\pi \ln\frac{m''^2_\pi}{\mu^2} + 2m''^4_\eta \ln\frac{m^2_\eta}{\mu^2} + 4m''^4_K \ln\frac{m^2_K}{\mu^2}\}. \tag{5.17}$$

For meson masses of O(500 *MeV*), $\mu \approx 1\,GeV$, $f \approx 150\,MeV$ and for quark masses such that $x \approx \frac{i}{f}$, the second term is O(10%) of the lowest order-term of $<\pi^0|\,0^{(8)}\,|K^0>$ proportional to a in (5.8) and the correction to the first term is of O(30%), indicating that chiral perturbation theory is valid for these parameters for this matrix element.

Corrections to (5.8) and (5.9) come from the diagrams in Fig. (12) and field renormalization. Assuming that all logarithms are of $O(\ln\frac{m^2_K}{\mu^2})$ the results are

$$<\pi^0|\,0^{(8)}\,|K^0> = \frac{-2\sqrt{2}a\,m'_\pi m'_K}{f^2}\{1 + \frac{1}{16\pi^2 f^2}\ln\frac{m'^2_K}{\mu^2}$$
$$\times[-\frac{17}{9}\frac{m'^3_K}{m'_\pi} - \frac{7}{6}m'^2_K + \frac{29}{9}m'_K m'_\pi - \frac{1}{2}m'^2_\pi]\}$$
$$+ \frac{\sqrt{2}b}{f^2}(m'_s + m'_d)\{1 + \frac{1}{16\pi^2 f^2}\ln\frac{m'^2_K}{\mu^2}$$
$$\times[-\frac{11}{18}m'^2_K + 3m'_\pi m'_K - \frac{7}{18}m'^2_\pi]\} \tag{5.18}$$
$$<\pi^0|\,0^{(27)}\,|K^0> = \frac{-4\sqrt{2}c}{f^2}m'''_K m'''_\pi\{1 - \frac{1}{16\pi^2 f^2}\ln\frac{m'''^2_K}{\mu^2}$$

$$\times[\frac{11}{2}m'''^2_K + 2m'''_K m'''_\pi + \frac{9}{2}m'''^2_\pi]\}\,. \qquad (5.19)$$

For the values mentioned earlier the corrections in (5.18) are O(5%) for the a term and O(20%) for the b term, indicating the validity of chiral perturbation theory. However, the corrections in (5.19) are large. To get a correction of O(30%) compared to tree level for $f \approx 150\,MeV$, $\mu \approx 1\,GeV$ we need to use meson masses of $O(150\,MeV)$ to calculate $<\pi^0|\,0'\,|K^0>$. Including one-loop corrections, eq. (5.12) is still valid with the following expressions for x and y[f1]:

$$x = \frac{i}{\sqrt{2}f}\frac{m'_s + m'_d}{m''_s - m''_d}\{1 + \frac{1}{16\pi^2 f^2}\ln\frac{m'^2_K}{\mu^2}\,[-\frac{11}{18}m'^2_K + 3m'_\pi m'_K - \frac{7}{18}m'^2_\pi]$$
$$+ \frac{1}{16\pi^2 f^2}\ln\frac{m''^2_K}{\mu^2}\,[\frac{13}{18}m''^2_\pi + \frac{29}{18}m''^2_K]\} \qquad (5.20)$$

$$y = \frac{m'''_\pi m'''_K}{m'_\pi m'_K}\{1 - \frac{1}{16\pi^2 f^2}\ln\frac{m_K^2}{\mu^2}\,\frac{113}{54}m_K^2$$
$$+ \frac{1}{16\pi^2 f^2}\ln\frac{m'^2_K}{\mu^2}\,[\frac{17}{9}\frac{m'^3_K}{m'_\pi} + \frac{7}{6}m'^2_K - \frac{29}{9}m'_K m'_\pi + \frac{1}{2}m'^2_\pi]$$
$$- \frac{1}{16\pi^2 f^2}\ln\frac{m''^2_K}{\mu^2}\,\frac{m'_K}{m'_\pi}[\frac{17}{9}m''^2_K + \frac{13}{9}m''^2_\pi]$$
$$+ \frac{1}{16\pi^2 f^2}\ln\frac{m'''^2_K}{\mu^2}\,[-\frac{11}{2}m'''^2_K - 2m'''_K m'''_\pi - \frac{9}{2}m'''^2_\pi]\}\,, \qquad (5.21)$$

which for the values mentioned earlier is a O(40%) correction to x and a O(50%) correction to y (with $m'''_K \sim 100\,MeV$), but the corrections to y depend crucially on using a small value for $m'''_{K,\pi}$.

The values of f used in (5.14-21) also have to be determined. We can do this in the standard way: measuring $<0\,|\,j_L^{\mu 1+i2}\,|\,\pi^+>$ where $j_L^{\mu a}$ is

[f1] In relation (5.20) we cannot use eq. (3.8) but we have to use the one-loop expressions to convert the quark mass ratios to meson mass rations from (3.36). We can however use it to get (5.21).

the left-handed current derived from the Lagrangian (3.6).

$$j_L^{\mu a} = -\frac{if^2}{4} tr(T^a \partial^\mu \Sigma \Sigma^\dagger) \text{ and } T^{1+i2} = \begin{bmatrix} 0 & 0 & 0 \\ 1 & 0 & 0 \\ 0 & 0 & 0 \end{bmatrix}. \quad (5.22)$$

We define f_π via

$$<0|j_L^{\mu 1+i2}|\pi^+> = -\frac{i}{2} f_\pi p_\pi^\mu . \quad (5.23)$$

Expanding (5.22) gives in lowest order $f = f_\pi$, but if we include the contribution from Fig. (13), with the square in Fig. (13) an insertion of $j_L^{\mu 1+i2}$, and field renormalization we get[f2]:

$$f_\pi = f\{1 + \frac{1}{16\pi^2 f^2}[-m_K^2 \ln \frac{m_K^2}{\mu^2} - 2m_\pi^2 \ln \frac{m_\pi^2}{\mu^2}]\} . \quad (5.24)$$

So the relation (5.11) can be used for determining $\Delta I = \frac{1}{2}$ enhancement provided we use meson masses of $0(500\,MeV)$ for $<\pi^0|0^{(8)}|K^0>$ and $<o|0^{(8)}|K^0>$ but use a smaller mass of $O(100\,MeV)$ to measure $<\pi^0|0^{(27)}|K^0>$. Then (5.11) will give the ratio $\frac{a}{2c}$ to about 40 ~ 50% depending on the value measured for $<o|0^{(8)}|K^0>$. The value of the $\Delta I = \frac{1}{2}$ part can be determined to within 40%, using meson masses of $0(500\,MeV)$ by eliminating a and b from eq. (5.14), (5.17) and (5.18) because it doesn't depend on the value of $<\pi^0|0^{(27)}|K^0>$.

[f2] See also Chapter III.

4. A test of the chiral limit on the lattice.

There exists another way to measure f on the lattice besides measuring (5.23). We can measure two matrix elements on the lattice of the operator

$$0'' = \bar{s}(1 - \gamma_5)d \ . \tag{5.25}$$

This is a divergence of a left-handed current for $m_s \neq m_d$ [26] and corresponds in chiral perturbation theory to the $(3_L, \bar{3}_R)$ operator

$$0'' = d\, tr\, A\Sigma \ , \tag{5.26}$$

with A given by (5.3).

At tree level $0''$ has matrix elements

$$<\pi^0|0''|K^0> = \frac{\sqrt{2}d}{f^2} \tag{5.27}$$

$$<o|0''|K^0> = \frac{2id}{f} \ . \tag{5.28}$$

Or at this order in chiral perturbation theory we can also determine f via the ratio

$$\frac{<o|0''|K^0>}{<\pi^0|0''|K^0>} = \sqrt{2}if \ . \tag{5.29}$$

Corrections to (5.27) come from the graphs in Figs. (12) and field renormalization; (5.28) gets corrections from Fig. (11) and field renormalization leading to[f3]

[f3] We could again use different meson masses for the various matrix elements.

$$<\pi^0|O''|K^0> = \frac{\sqrt{2}d}{f^2}\{1 + \frac{1}{16\pi^2 f^2}\ln\frac{m_K^2}{\mu^2}\,[-\frac{11}{18}m_K^2 + 3m_K m_\pi - \frac{7}{18}m_\pi^2]\}$$

(5.30)

$$<o|O''|K^0> = \frac{2id}{f}\{1 - \frac{1}{16\pi^2 f^2}\ln\frac{m_K^2}{\mu^2}\,[\frac{29}{18}m_K^2 + \frac{13}{18}m_\pi^2]\}\,. \quad (5.31)$$

Both corrections are 0(25%) or less for the values of the parameters used earlier and lead to

$$\frac{<o|O''|K^0>}{<\pi^0|O''|K^0>} = \sqrt{2}if' = \sqrt{2}if\{1 + \frac{1}{16\pi^2 f^2}\ln\frac{m_K^2}{\mu^2}[-m_K^2 - 3m_K m_\pi - \frac{1}{3}m_\pi^2]\}\,.$$

(5.32)

So measuring f via f_π or via f' should differ by

$$\frac{f'}{f_\pi} = 1 - \frac{1}{16\pi^2 f^2}\ln\frac{m_K^2}{\mu^2}\,[3m_K m_\pi - \frac{5}{3}m_\pi^2]\,. \quad (5.33)$$

Or they differ by 0(12%) using the same parameters as before. This relation provides excellent means to determine the accuracy of chiral perturbation theory on the lattice since it has small corrections. Present lattice calculations, however, seem to be quite far from this point [26].

VI. CHIRAL PERTURBATION THEORY AND HYPERON DECAYS.

1. Introduction

The results of this chapter can be found in [30]. In this chapter we have $m_u=m_d=0$ which is a good approximation for real particles. Lowest-order chiral perturbation theory makes predictions for the weak nonleptonic decays of hyperons. Experimentally, the predictions of lowest-order chiral perturbation theory work well for the *S*-wave hyperon decay amplitudes but fail badly for the *P*-wave hyperon decay amplitudes. In this chapter the leading corrections to lowest-order chiral perturbation theory for nonleptonic hyperon decays are computed. These corrections arise from one-loop contributions to hyperon decay amplitudes. For the *P*-wave amplitudes we find that the corrections to lowest-order chiral perturbation theory are large, indicating a breakdown of chiral perturbation theory for these amplitudes. This is consistent with the experimental failure of the predictions of lowest-order chiral perturbation theory for the *P*-wave amplitudes. Unfortunately, we find that some of the *S*-wave hyperon decay amplitudes also get large corrections. In particular, the Lee-Sugawara relation [32] gets a large correction indicating a breakdown of chiral perturbation theory for this relation.

In Section 2 the chiral Lagrangian for the strong interactions of the baryons and the pseudo-Goldstone bosons is given. The determination of the parameters in this Lagrangian, to lowest-order in chiral perturbation theory, is reviewed. The leading corrections to the predictions of

lowest-order chiral perturbation theory for these parameters are computed.

Section 3 contains a discussion of weak nonleptonic hyperon decays. The predictions of lowest-order chiral perturbation theory are reviewed and the leading corrections to these predictions are computed.

2. Chiral perturbation theory for baryon-meson strong interactions

The strong interactions of the pseudo-Goldstone bosons at low momentum are described by an effective field theory that transforms correctly under chiral $SU(3)_L \times SU(3)_R$ symmetry and is invariant under parity and charge conjugation. The pseudo-Goldstone boson fields are incorporated in a 3×3 special unitary matrix

$$\Sigma = \exp \frac{2iM}{f}, \tag{6.1}$$

where

$$M = \begin{bmatrix} \frac{1}{\sqrt{2}}\pi^0 + \frac{1}{\sqrt{6}}\eta & \pi^+ & K^+ \\ \pi^- & -\frac{1}{\sqrt{2}}\pi^0 + \frac{1}{\sqrt{6}}\eta & K^0 \\ K^- & \bar{K}^0 & -\left(\frac{2}{3}\right)^{\frac{1}{2}}\eta \end{bmatrix}. \tag{6.2}$$

Under an $SU(3)_L \times SU(3)_R$ transformation

$$\Sigma \rightarrow L \Sigma R^{\dagger}, \tag{6.3}$$

with $L \varepsilon SU(3)_L$ and $R \varepsilon SU(3)_R$. We are interested in the interactions of the pseudo-Goldstone bosons with baryons. The baryon fields are incorporated in the 3×3 matrix

$$B = \begin{bmatrix} \frac{1}{\sqrt{2}}\Sigma^0 + \frac{1}{\sqrt{6}}\Lambda & \Sigma^+ & p \\ \Sigma^- & -\frac{1}{\sqrt{2}}\Sigma^0 + \frac{1}{\sqrt{6}}\Lambda & n \\ \Xi^- & \Xi^0 & -\left(\frac{2}{3}\right)^{\frac{1}{2}}\Lambda \end{bmatrix}. \tag{6.4}$$

Under an $SU(3)_L \times SU(3)_R$ transformation

$$B \to UBU^\dagger. \tag{6.5}$$

Here U is a 3×3 unitary matrix defined by the transformation properties of

$$\xi = \exp \frac{iM}{f} = \sqrt{\Sigma}. \tag{6.6}$$

Under an $SU(3)_L \times SU(3)_R$ transformation

$$\xi \to L\xi U^\dagger = U\xi R^\dagger, \tag{6.7}$$

where $L \varepsilon SU(3)_L$ and $R \varepsilon SU(3)_R$. Note that U is a nonlinear function of L,R and M. Therefore, U depends on space-time coordinates.

In lowest-order chiral perturbation theory the strong interactions of the pseudo-Goldstone bosons and baryons are described by the effective Lagrangian density

$$L = L_0 + L_1. \tag{6.8}$$

The Lagrangian density

$$\begin{aligned} L_0 = {} & \frac{f^2}{8} Tr\, \partial_\mu \Sigma \partial^\mu \Sigma^\dagger + Tr\, \bar{B} i\not{\partial} B - M Tr\, \bar{B} B \\ & + \frac{i}{2} Tr\, \bar{B} \gamma^\mu [\xi \partial_\mu \xi^\dagger + \xi^\dagger \partial_\mu \xi, B] \\ & + \frac{iD}{2} Tr\, \bar{B} \gamma^\mu \gamma_5 \{\xi \partial_\mu \xi^\dagger - \xi^\dagger \partial_\mu \xi, B\} \\ & + \frac{iF}{2} Tr\, \bar{B} \gamma^\mu \gamma_5 [\xi \partial_\mu \xi^\dagger - \xi^\dagger \partial_\mu \xi, B], \end{aligned} \tag{6.9}$$

is invariant under $SU(3)_L \times SU(3)_R$. The Lagrangian density L_1 is

proportional to the quark-mass matrix. Neglecting up and down quark masses the mass matrix is

$$m = \begin{bmatrix} 0 & 0 & 0 \\ 0 & 0 & 0 \\ 0 & 0 & m_s \end{bmatrix}. \tag{6.10}$$

The Lagrangian density L_1 transforms like $(\bar{3},3) + (3,\bar{3})$ under $SU(3)_L \times SU(3)_R$ and is given by [f1]

$$L_1 = a_1 tr(m\Sigma + m\Sigma^\dagger) + b_1 Tr\,\bar{B}(\xi^\dagger m\,\xi^\dagger + \xi m\,\xi)B$$

$$+ b_2 Tr\,\bar{B}B(\xi^\dagger m\,\xi^\dagger + \xi m\,\xi). \tag{6.11}$$

The left-handed current can be derived from L using the Noether procedure. For this purpose it is convenient to express the chiral Lagrangian in terms of the baryon fields

$$\tilde{B}_L = \frac{1}{2}\,(1-\gamma_5)\xi B\xi^\dagger \tag{6.12a}$$

$$\tilde{B}_R = \frac{1}{2}\,(1+\gamma_5)\xi^\dagger B\xi, \tag{6.12b}$$

since they transform in the simple manner,

$$\tilde{B}_L \to L\tilde{B}_L L^\dagger \text{ and } \tilde{B}_R \to R\tilde{B}_R R^\dagger, \tag{6.13}$$

[f1] The terms $Tr\,\bar{B}\gamma_5(\xi^\dagger m\xi^\dagger - \xi m\xi)B$ and $Tr\bar{B}\gamma_5 B(\xi^\dagger m\xi^\dagger - \xi m\xi)$ are suppressed because $\bar{B}\gamma_5 B$ vanishes for baryons at rest.

under $SU(3)_L \times SU(3)_R$. Using this technique we find that the left-handed current is

$$J_\mu^a = -\frac{1}{2} Tr\, \bar{B}\gamma_\mu[\xi^\dagger T^a \xi, B] + \frac{1}{2} D\, Tr\, \bar{B}\gamma_\mu\gamma_5\{\xi^\dagger T^a \xi, B\}$$
$$+ \frac{1}{2} F\, Tr\, \bar{B}\gamma_\mu\gamma_5[\xi^\dagger T^a \xi, B] - \frac{if^2}{4} Tr\,(\partial_\mu \Sigma)\Sigma^\dagger T^a. \qquad (6.14)$$

Matrix elements of J_μ^{4+i5} between baryon states are measured in semileptonic hyperon decays. The matrix element of J_μ^{1+i2} between the neutron and proton is measured in neutron beta decay. In the leading order of chiral perturbation theory these matrix elements follow from a tree level evaluation of matrix elements of the current in eq. (6.14). Explicitly, [f2]

$$\langle p | J_\mu^{1+i2} | n \rangle = \frac{1}{2} \bar{u}_p \{-\gamma_\mu + (D+F)\gamma_\mu\gamma_5\} u_n, \qquad (6.15a)$$

$$\langle \Lambda | J_\mu^{1+i2} | \Sigma^- \rangle = \frac{1}{\sqrt{6}} \bar{u}_\Lambda \{0\gamma_\mu + D\gamma_\mu\gamma_5\} u_{\Sigma^-}, \qquad (6.15b)$$

$$\langle p | J_\mu^{4+i5} | \Lambda \rangle = \frac{1}{2\sqrt{6}} \bar{u}_p \{3\gamma_\mu - (D+3F)\gamma_\mu\gamma_5\} u_\Lambda, \qquad (6.15c)$$

$$\langle \Lambda | J_\mu^{4+i5} | \Xi^- \rangle = \frac{1}{2\sqrt{6}} \bar{u}_\Lambda \{-3\gamma_\mu - (D-3F)\gamma_\mu\gamma_5\} u_{\Xi^-}, \qquad (6.15d)$$

$$\langle n | J_\mu^{4+i5} | \Sigma^- \rangle = \frac{1}{2} \bar{u}_n \{\gamma_\mu + (D-F)\gamma_\mu\gamma_5\} u_{\Sigma^-}, \qquad (6.15e)$$

$$\langle \Sigma^0 | J_\mu^{4+i5} | \Xi^- \rangle = \frac{1}{2\sqrt{2}} \bar{u}_{\Sigma^0} \{-\gamma_\mu + (D+F)\gamma_\mu\gamma_5\} u_{\Xi^-}. \qquad (6.15f)$$

A fit to semileptonic hyperon decays gives $F = 0.44$ and $D=0.81$ [29]. Evaluating the tree level matrix element of the left-handed current J_μ^{1+i2} in eq. (6.14) between a π^+ and the vacuum gives that

[f2] In (6.15) u_B denotes a spinor for baryon B and $\bar{u}_B = u_B^\dagger \gamma^0$.

$$f = f_\pi \approx 134 \text{ MeV}. \tag{6.16}$$

Evaluating the masses of the mesons and baryons at tree level, we find

$$m_K^2 = \frac{3}{4}\, m_\eta^2 = \frac{4 a_1}{f^2}\, m_s, \tag{6.17}$$

$$M_N = M - 2b_2\, m_s, \tag{6.18a}$$

$$M_\Sigma = M, \tag{6.18b}$$

$$M_\Lambda = M - \frac{4}{3}\,(b_1 + b_2) m_s, \tag{6.18c}$$

$$M_\Xi = M - 2b_1 m_s. \tag{6.18d}$$

These equations determine the values of the parameters $M, a_1 m_s$, $b_1 m_s$ and $b_2 m_s$ to leading order in chiral perturbation theory. Combining baryon masses to eliminate b_1 and b_2 gives the Gell-Mann-Okubo relation for the baryon masses [28]

$$\frac{3}{4}\, M_\Lambda + \frac{1}{4}\, M_\Sigma - \frac{1}{2}\,(M_N + M_\Xi) = 0. \tag{6.19}$$

The leading corrections to the current matrix elements in eqs. (6.15) are of order $m_s \ln m_s$. These arise from a one-loop evaluation of the matrix elements of the left-handed current in eq. (6.14). This correction dominates over the corrections of order m_s because of the "large" logarithm. The corrections of order m_s are not computable since they can arise from a tree level evaluation of matrix elements of higher-derivative operators in the left-handed current. Only the axial part of the left-handed current, A_μ^a, defined by $J_\mu^a = V_\mu^a - A_\mu^a$, gets

corrections of order $m_s \ln m_s$. The Feynman diagrams which give nonzero corrections of this order to the axial current are shown in Fig. (13). Parameterizing these corrections in the form

$$\Delta \langle B_f | A_\mu^a | B_i \rangle = - \alpha^a_{B_f B_i} \frac{m_K^2}{(4\pi f)^2} \ln(m_K^2/\mu^2)\, \bar{u}_{B_f} \gamma_\mu \gamma_5 u_{B_i}, \qquad (6.20)$$

we find that

$$\alpha_{pn}^{1+i2} = \frac{2}{9} D^3 + \frac{2}{9} D^2F + \frac{2}{3} DF^2 - 2F^3 - \frac{1}{2} D - \frac{1}{2} F \qquad (6.21a)$$

$$\alpha_{\Lambda\Sigma^-}^{1+i2} = \frac{1}{\sqrt{6}} \left(\frac{17}{9} D^3 - DF^2 - D \right) \qquad (6.21b)$$

$$\alpha_{p\Lambda}^{4+i5} = \frac{1}{\sqrt{6}} \left(\frac{19}{18} D^3 - \frac{5}{2} D^2F - \frac{7}{2} DF^2 + \frac{9}{2} F^3 + \frac{5}{4} D + \frac{15}{4} F \right) \qquad (6.21c)$$

$$\alpha_{\Lambda\Xi^-}^{4+i5} = \frac{1}{\sqrt{6}} \left(\frac{19}{18} D^3 + \frac{5}{2} D^2F - \frac{7}{2} DF^2 - \frac{9}{2} F^3 + \frac{5}{4} D - \frac{15}{4} F \right) \qquad (6.21d)$$

$$\alpha_{n\Sigma^-}^{4+i5} = \frac{7}{18} D^3 - \frac{13}{18} D^2F + \frac{7}{6} DF^2 + \frac{1}{2} F^3 - \frac{5}{4} D + \frac{5}{4} F \qquad (6.21e)$$

$$\alpha_{\Sigma^0\Xi^-}^{4+i5} = \frac{1}{\sqrt{2}} \left(\frac{7}{18} D^3 + \frac{13}{18} D^2F + \frac{7}{6} DF^2 - \frac{1}{2} F^3 - \frac{5}{4} D - \frac{5}{4} F \right). \qquad (6.21f)$$

These corrections are quite small. For a subtraction point $\mu = 1$ GeV, none of these corrections exceeds 30% of the leading contribution.

The leading and next-to-leading corrections to the baryon mass formulae in eqs. (6.18) are of order $m_s^{3/2}$ [16] and $m_s^2 \ln m_s$, respectively. They arise from the one-loop Feynman diagram in Fig. (15a), which contributes directly to the mass, and from the one-loop Feynman diagram in Fig. (15b), which contributes directly to the mass and indirectly through wave-function renormalization of the baryon fields. Parameterizing these corrections to the baryon masses in the form

$$\Delta M_B = \frac{\eta_B m_K^3}{8\pi f^2} + \frac{\gamma_B m_K^2 m_s}{(4\pi f)^2} \ln (m_K^2/\mu^2), \tag{6.22}$$

we have

$$\eta_N = -\left\{\left[\frac{5}{3} + \frac{4\sqrt{3}}{27}\right] D^2 - \left[2 + \frac{8\sqrt{3}}{9}\right] DF + \left[3 + \frac{4\sqrt{3}}{3}\right] F^2\right\}, \tag{6.23a}$$

$$\eta_\Sigma = -\left\{\left[2 + \frac{16\sqrt{3}}{27}\right] D^2 + 2F^2\right\}, \tag{6.23b}$$

$$\eta_\Lambda = -\left\{\left[\frac{2}{3} + \frac{16\sqrt{3}}{27}\right] D^2 + 6F^2\right\}, \tag{6.23c}$$

$$\eta_\Xi = -\left\{\left[\frac{5}{3} + \frac{4\sqrt{3}}{27}\right] D^2 + \left[2 + \frac{8\sqrt{3}}{9}\right] DF + \left[3 + \frac{4\sqrt{3}}{3}\right] F^2\right\}, \tag{6.23d}$$

and

$$\gamma_N = \left\{2b_1 + \frac{68}{9} b_2 + b_2\left[\frac{28}{3} D^2 - 16DF + 12F^2\right] - b_1\left[\frac{2}{3} D^2 + 4DF + 6F^2\right]\right\}, \tag{6.24a}$$

$$\gamma_\Sigma = \left\{2b_1 + 2b_2 - 6b_2 (D - F)^2 - 6b_1 (D + F)^2\right\}, \tag{6.24b}$$

$$\gamma_\Lambda = \left\{\frac{154}{27} (b_1 + b_2) + b_2\left[\frac{2}{3} D^2 - 12DF + 6F^2\right] + b_1\left[\frac{2}{3} D^2 + 12DF + 6F^2\right]\right\}, \tag{6.24c}$$

$$\gamma_\Xi = \left\{\frac{68}{9} b_1 + 2b_2 - b_2\left[\frac{2}{3} D^2 - 4DF + 6F^2\right] + b_1\left[\frac{28}{3} D^2 + 16DF + 12F^2\right]\right\}. \tag{6.24d}$$

The corrections η_B were calculated previously in Ref. [16]. Our results disagree with those in Ref. [16][f3]. The corrections in eqs. (6.23)

[f3] We also calculated η_B from the divergence of the vector current. This was the method used in Ref. [16].

and (6.24) change the Gell-Mann-Okubo relation to:

$$\frac{3}{4} M_\Lambda + \frac{1}{4} M_\Sigma - \frac{1}{2}(M_N + M_\Xi)$$
$$= \frac{m_K^3}{12\pi f^2}\left[1 - \frac{2}{\sqrt{3}}\right](D^2 - 3F^2) - 4D^2(M_\Sigma - M_\Lambda)\frac{m_K^2}{(4\pi f)^2}\ln\left[\frac{m_K^2}{\mu^2}\right]. \tag{6.25}$$

The first term on the left-hand side of eq. (6.25) is extremely small and the second term on the left-hand side of eq. (6.25) is about 26 MeV for a subtraction point $\mu = 1$ GeV. Experimentally, $3/4\,M_\Lambda + 1/4\,M_\Sigma - 1/2\,(M_N + M_\Xi) \approx 6.5$ MeV.

Finally, we note that there is a one-loop correction to the matrix element of the left-handed current J_μ^{1+i2} between a π^+ and the vacuum which gives [16]

$$f = f_\pi\left[1 + \frac{m_K^2}{(4\pi f)^2}\ln\frac{m_K^2}{\mu^2}\right]. \tag{6.26}$$

3. Chiral perturbation theory for weak nonleptonic hyperon decays

The Hamiltonian for weak nonleptonic hyperon decays transforms like $(8_L,1_R) + (27_L,1_R)$ under chiral $SU(3)_L \times SU(3)_R$. Experiments indicate that the $(8_L,1_R)$ part of the effective Hamiltonian dominates the decay amplitudes. In the leading order of chiral perturbation theory the $(8_L,1_R)$ effective Hamiltonian density for $|\Delta S| = 1$ weak nonleptonic decays is

$$H_{eff}^{|\Delta S| = 1} = a\ Tr\ \bar{B}\left\{\xi^\dagger h\, \xi, B\right\} + b\ Tr\ \bar{B}[\xi^\dagger h\, \xi, B] + h.c., \qquad (6.27)$$

where

$$h = \begin{bmatrix} 0 & 0 & 0 \\ 0 & 0 & 1 \\ 0 & 0 & 0 \end{bmatrix}, \qquad (6.28)$$

projects out the correct component of the octet. The invariant matrix elements for nonleptonic hyperon decays have the form

$$M(B_i \to B_f \pi) = \bar{u}_{B_f} \left\{ A^{(S)}\,(B_i \to B_f \pi) + \gamma_5\, A^{(P)}\,(B_i \to B_f \pi) \right\} u_{B_i}. \qquad (6.29)$$

The parameters $A^{(S)}(B_i \to B_f \pi)$ and $A^{(P)}(B_i \to B_f \pi)$ specify the S-wave and P-wave amplitudes, respectively. Isospin symmetry of the strong interactions implies that

$$M(\Lambda \to p\pi^-) + \sqrt{2}\, M(\Lambda \to n\pi^0) = 0, \qquad (6.30a)$$

$$M(\Xi^- \to \Lambda\pi^-) + \sqrt{2}\, M(\Xi^0 \to \Lambda\pi^0) = 0, \qquad (6.30b)$$

$$\sqrt{2}\, M(\Sigma^+ \to p\pi^0) + M(\Sigma^- \to n\pi^-) - M(\Sigma^+ \to n\pi^+) = 0. \qquad (6.30c)$$

The isospin relations (6.30) hold for both the S-wave and P-wave decay amplitudes.

The decay amplitudes for $\Sigma^+ \to n\pi^+$, $\Sigma^- \to n\pi^-$, $\Xi^- \to \Lambda\pi^-$ and $\Lambda \to p\pi^-$ are not related by isospin. Evaluating tree level matrix elements of the effective Hamiltonian density (6.27) gives the leading predictions of chiral perturbation theory for these amplitudes. Explicitly for the S-wave amplitudes [31]

$$A^{(S)}(\Sigma^+ \to n\pi^+) = 0, \tag{6.31a}$$

$$A^{(S)}(\Sigma^- \to n\pi^-) = \frac{a-b}{f}, \tag{6.31b}$$

$$A^{(S)}(\Lambda \to p\pi^-) = -\frac{a+3b}{\sqrt{6}f}, \tag{6.31c}$$

$$A^{(S)}(\Xi^- \to \Lambda\pi^-) = \frac{3b-a}{\sqrt{6}f}. \tag{6.31d}$$

A least-squares fit to the seven measured S-wave amplitudes gives a = 0.56 and b = - 1.42 in units of $G_F m_{\pi^+}^2 f_\pi$. For the P-wave amplitudes the pole diagrams in Fig. (16) give [31]

$$A^{(P)}(\Sigma^+ \to n\pi^+) = \frac{2M_N}{f}\left\{\frac{D(a-b)}{M_\Sigma - M_N} + \frac{D(a/3+b)}{M_\Lambda - M_N}\right\}, \tag{6.32a}$$

$$A^{(P)}(\Sigma^- \to n\pi^-) = \frac{2M_N}{f}\left\{\frac{F(a-b)}{M_\Sigma - M_N} + \frac{D(a/3+b)}{M_\Lambda - M_N}\right\}, \tag{6.32b}$$

$$A^{(P)}(\Lambda \to p\pi^-) = \frac{2M_N}{\sqrt{6}f}\left\{\frac{(-a-3b)(D+F)}{M_\Lambda - M_N} + \frac{2(b-a)D}{M_\Sigma - M_N}\right\}, \tag{6.32c}$$

$$A^{(P)}(\Xi^- \to \Lambda\pi^-) = \frac{2M_\Lambda}{\sqrt{6}f}\left\{\frac{(a-3b)(D-F)}{M_\Xi - M_\Lambda} + \frac{2D(a+b)}{M_\Xi - M_\Sigma}\right\}. \tag{6.32d}$$

The parameters $A^{(P)}$ have differences of baryon masses in the denominator because they arise from pole diagrams. Although the parameters $A^{(P)}$ are proportional to $1/m_s$, in the leading order of chiral

perturbation theory, the P-wave decay amplitudes (like the S-wave decay amplitudes) are independent of the strange quark mass because $\bar{u}_{B_f}\gamma_5 u_{B_i}$ is proportional to m_s.

Note that the expressions for the parameters $A^{(S,P)}(\Lambda \to p\pi^-)$ can be deduced from those for $A^{(S,P)}(\Xi^- \to \Lambda\pi^-)$ by the change of variables: $M_\Xi \to M_N$, $b \to -b$ and $F \to -F$. This occurs because the Lagrangians for the strong interactions in eqs. (6.9) and (6.11) and the Hamiltonian for weak interactions in eq. (6.27) are invariant under[f4]

$$M \to M^T, \quad B \to B^T, \quad \bar{B} \to \bar{B}^T, \tag{6.33}$$

provided we flip the sign of F, interchange b_1 and b_2 and flip the sign of b. Since eq. (6.33) interchanges p with Ξ^-, and π^+ with π^-, crossing symmetry implies the relation between $A^{(S,P)}(\Lambda \to p\pi^-)$ and $A^{(S,P)}(\Xi^- \to \Lambda\pi^-)$.

The S-wave amplitudes in eqs. (6.31) can be combined to eliminate a and b. This yields the Lee-Sugawara relation [32]

$$A^{(S)}(\Lambda \to p\pi^-) + 2\,A^{(S)}(\Xi^- \to \Lambda\pi^-) + \left[\frac{2}{3}\right]^{\frac{1}{2}} A^{(S)}(\Sigma^- \to n\pi^-) = 0. \tag{6.34}$$

The leading corrections to lowest-order chiral perturbation theory for hyperon decay amplitudes are of order $m_s \ln m_s$. These arise from a one-loop evaluation of the matrix elements of the effective Hamiltonian in eq. (6.27). The corrections of order $m_s \ln m_s$ dominate over those of order m_s because of the "large" logarithm. The corrections of order m_s

[f4] This "symmetry" can also be seen in the matrix elements of the currents and the baryon masses. The "symmetry" generalizes to higher derivative operators.

are not computable since they can arise from subleading operators in the effective Hamiltonian for $|\Delta S| = 1$ weak nonleptonic decays that involve a derivative or a factor of the quark mass matrix.

The one-loop Feynman diagrams which give a nonzero contribution of order $m_s \ln m_s$ to the S-wave decay amplitudes are shown in Fig. (17)[f5]. In Fig. (17) a shaded square denotes a vertex from the weak interaction Hamiltonian eq. (6.27), while a shaded circle denotes a strong interaction vertex from eq. (6.9). Writing the corrections to the S-wave amplitudes in the form

$$\Delta A^{(S)}(B_i \to B_f \pi) = \varphi_{B_i B_f} \frac{m_K^2}{(4\pi f)^2} \ln(m_K^2/\mu^2), \tag{6.35}$$

we find that

$$\varphi_{\Sigma^+ n} = 0, \tag{6.36a}$$

$$\varphi_{\Sigma^- n} = \frac{a}{f}\left(-\frac{3}{2} - \frac{7}{3} D^2 + 6DF + 3F^2\right) - \frac{b}{f}\left(-\frac{3}{2} + \frac{5}{3} D^2 + 10DF + 3F^2\right), \tag{6.36b}$$

$$\varphi_{\Lambda p} = -\frac{a}{\sqrt{6}f}\left(-\frac{3}{2} + \frac{19}{3} D^2 - 22DF + 9F^2\right) - \frac{3b}{\sqrt{6}f}\left(-\frac{3}{2} + \frac{7}{3} D^2 - 10DF + 9F^2\right), \tag{6.36c}$$

$$\varphi_{\Xi^- \Lambda} = -\frac{a}{\sqrt{6}f}\left(-\frac{3}{2} + \frac{19}{3} D^2 + 22DF + 9F^2\right) + \frac{3b}{\sqrt{6}f}\left(-\frac{3}{2} + \frac{7}{3} D^2 + 10DF + 9F^2\right). \tag{6.36d}$$

[f5] There is also a correction from pion wave function renormalization. Baryon wave function renormalization does not contribute at order $m_s \log m_s$.

The dependence of the corrections (6.35) on the subtraction point μ is canceled by the contribution of operators with one insertion of the quark-mass matrix [12]. However, none of the subleading operators with a single insertion of the quark mass matrix contribute to $\Sigma^+ \to n\pi^+$. This explains the vanishing of $\varphi_{\Sigma^+ n}$. Note, however, that this does not mean that there are no contributions to $A^{(S)}(\Sigma^+ \to n\pi^+)$ of order m_s. There are subleading operators with a derivative that give such a contribution[f6].

For a subtraction point $\mu = 1$ GeV table 3 gives the corrections to the S-wave amplitudes. The $\Sigma^- \to n\pi^-$ and $\Lambda \to p\pi^-$ corrections are about 30% of the leading contribution. However, the correction to the S-wave amplitude for $\Xi^- \to \Lambda\pi^-$ is large, indicating a breakdown of chiral perturbation theory for this S-wave amplitude. The corrections (6.36) change the Lee-Sugawara relation to

$$A^{(S)}(\Lambda \to p\pi^-) + 2A^{(S)}(\Xi^- \to \Lambda\pi^-) + \left[\frac{3}{2}\right]^{\frac{1}{2}} A^{(S)}(\Sigma^- \to n\pi^-)$$

$$= -\frac{1}{\sqrt{6}f} \frac{m_K^2 \ln(m_K^2/\mu^2)}{(4\pi f)^2} \left\{ a(26D^2 + 4DF + 18F^2) + b(-2D^2 - 60DF - 18F^2) \right\}. \tag{6.37}$$

The large discrepancy between eqs. (6.37) and (6.34) indicates that chiral perturbation theory for the Lee-Sugawara relation has broken down.

The Feynman diagrams which give a nonzero contribution of order $m_s \ln m_s$ to the P-wave decay amplitudes are shown in Figs. (18)[f7].

[f6] For example : $Tr(\bar{B}\gamma^\mu \xi \partial_\mu \Sigma^\dagger \xi B \xi^\dagger h \xi)$.

Again, a shaded square denotes a weak interaction vertex from (6.27) and a shaded circle denotes a strong interaction vertex from eq. (6.9). Writing the correction of order $m_s \ln m_s$ in the form

$$\Delta A^{(P)}(B_i \to B_f \pi) = \omega_{B_i B_f} \frac{m_K^2}{(4\pi f)^2} \ln(m_K^2/\mu^2), \tag{6.38}$$

we find that

$$\begin{aligned}\omega_{\Sigma^+ n} = \frac{2M_N}{f(M_\Sigma - M_N)} \Big\{ a \Big[&- \frac{5}{2} D - \frac{17}{9} D^3 + \frac{19}{3} D^2 F + \frac{13}{3} DF^2 - 3F^3 \Big] \\ &- b \Big[- \frac{5}{2} D + \frac{19}{9} D^3 + \frac{31}{3} D^2 F + \frac{13}{3} DF^2 - 3F^3 \Big] \Big\} \\ + \frac{2M_N}{f(M_\Lambda - M_N)} \Big\{ &\frac{a}{3} \Big[- \frac{5}{2} D + \frac{74}{9} D^3 - 22 D^2 F + 8 DF^2 \Big] \\ &+ b \Big[- \frac{5}{2} D + \frac{38}{9} D^3 - 10 D^2 F + 8 DF^2 \Big] \Big\} \end{aligned} \tag{6.39a}$$

$$\begin{aligned}\omega_{\Sigma^- n} = \frac{2M_N}{f(M_\Sigma - M_N)} \Big\{ a \Big[&- \frac{5}{2} F - \frac{20}{9} D^2 F + 6 DF^2 + 2F^3 \Big] \\ &- b \Big[- \frac{5}{2} F + \frac{16}{9} D^2 F + 10 DF^2 + 2F^3 \Big] \Big\} \\ + \frac{2M_N}{f(M_\Lambda - M_N)} \Big\{ &\frac{a}{3} \Big[- \frac{5}{2} D + \frac{74}{9} D^3 - 22 D^2 F + 8 DF^2 \Big] \\ &+ b \Big[- \frac{5}{2} D + \frac{38}{9} D^3 - 10 D^2 F + 8 DF^2 \Big] \Big\} \end{aligned} \tag{6.39b}$$

$$\omega_{\Lambda p} = \frac{2M_N}{\sqrt{6} f(M_\Lambda - M_N)} \Big\{ - a \Big[- \frac{5}{2}(D+F) + \frac{61}{9} D^3 - \frac{137}{9} D^2 F - \frac{35}{3} F^2 D + 5F^3 \Big]$$

[17] There is also a correction from pion field renormalization. Baryon field renormalization does not contribute at this order.

$$- 3b\left[-\frac{5}{2}(D+F) + \frac{25}{9}D^3 - \frac{65}{9}D^2F + \frac{1}{3}F^2D + 5F^3\right]\Bigg\}$$
$$+ \frac{2M_N}{\sqrt{6}f(M_\Sigma - M_N)}\left\{-2a\left[-\frac{5}{2}D - \frac{4}{9}D^3 + 6D^2F + 2DF^2\right]\right.$$
$$\left. + 2b\left[-\frac{5}{2}D + \frac{32}{9}D^3 + 10D^2F + 2DF^2\right]\right\} \qquad (6.39c)$$

$$\omega_{\Xi^-\Lambda} = \frac{2M_\Lambda}{\sqrt{6}f(M_\Xi - M_\Lambda)}\left\{a\left[-\frac{5}{2}(D-F) + \frac{61}{9}D^3 + \frac{137}{9}D^2F - \frac{35}{3}DF^2 - 5F^3\right]\right.$$
$$\left. - 3b\left[-\frac{5}{2}(D-F) + \frac{25}{9}D^3 + \frac{65}{9}D^2F + \frac{1}{3}DF^2 - 5F^3\right]\right\}$$
$$+ \frac{2M_\Lambda}{\sqrt{6}f(M_\Xi - M_\Sigma)}\left\{2a\left[-\frac{5}{2}D - \frac{4}{9}D^3 - 6D^2F + 2DF^2\right]\right.$$
$$\left. + 2b\left[-\frac{5}{2}D + \frac{32}{9}D^3 - 10D^2F + 4DF^2\right]\right\}. \qquad (6.39d)$$

As shown in Table 3, for a subtraction point μ= 1 GeV, these corrections are large, indicating a breakdown of chiral perturbation theory for the P-wave amplitudes[f8]. It appears that the puzzling feature of nonleptonic hyperon decays is not the failure of the predictions of lowest-order chiral perturbation theory for the P-wave amplitudes[f9] but rather the success of the Lee-Sugawara relation for S-wave amplitudes.

[f8] The leading order P-wave results (6.32) and the corrections (6.39) are very sensitive to the values of F,D,a and b. However, for any reasonable values of these parameters the corrections are large.

[f9] For an explanation of the failure of chiral perturbation theory for the P-wave amplitudes in the chiral quark model see [10,13].

VII. THE SOLITON MODEL OF BARYONS.

1. Introduction.

The results of this Chapter are published in [40]. The strong interaction chiral Lagrangian (3.6a), in general, possesses static solutions to its equations of motion. Due to the presence of higher derivative terms these solutions of the equations of motion can be stable[33]. The Wess-Zumino term, which is added to the action to include the effects of anomalies[34], implies that these solitons are baryons[35].

These solutions still include the effects of the $SU(3)_L \times SU(3)_R$ symmetry. All the results of the previous Chapter are thus still valid in the soliton model. The soliton model allows, however, for some predictions beyond those of the previous Chapter.

In the rest of this Section we will briefly describe the soliton model. In the next Section we derive F/D for nonleptonic hyperon S-wave decays, in Section 3 F/D for semileptonic hyperon decays and in Section 4 F/D for hyperon magnetic moments.

The soliton solutions have the form

$$\Sigma(x)=A\Sigma_0(x)A^{\dagger}, \tag{7.1}$$

where A is a 3×3 special unitary matrix and

$$\Sigma_0(x)=\begin{pmatrix} \exp(-iF(r)\hat{x}\cdot\sigma) & 0 \\ 0 & 1 \end{pmatrix}, \tag{7.2}$$

with $F(0)=\pi$ and $F(\infty)=0$. In the semiclassical approximation the soliton is treated as having a large mass but a fixed size. Then the higher-order time derivatives in the strong Lagrangian are suppressed. Note, however, that for baryons there is no sense in which the higher-order spatial derivatives are negligible. This semiclassical picture for baryons coincides with the large N_c limit where baryons are heavy because they contain a large number of quarks, but their size is fixed by the confinement scale[36].

The effective Lagrangian in (3.6a) thus describes the strong interactions of the Goldstone bosons and baryons at low momenta. Quantization about the soliton solution is achieved by treating the collective coordinate A as a dynamical variable. The wave functions for the baryons take the form[37]

$$\psi(A)=\sum_{n}\sum_{ab} C_{ab}^{(n)} D_{ab}^{(n)}(A), \tag{7.3}$$

where $D_{ab}^{(n)}(A)$ is the unitary matrix for the representation (n) of the $SU(3)$ transformation A. Each subscript is determined by a set of three numbers : $a=(a_1, a_2, a_3)$ and $b=(b_1, b_2, b_3)$. The index a determines the hypercharge and isospin quantum numbers

$$(a_1, a_2, a_3)=(Y, I, I_3), \tag{7.4}$$

while the index b determines the spin quantum numbers

$$(b_1, b_2, _3)=(1, S, S_3). \tag{7.5}$$

The Wess-Zumino term fixes b_1, since right multiplication of A by $U(1)$ transformations generated by λ^8 do not alter the soliton

solution[37].

2. *F/ D* for nonleptonic hyperon decays.

The effective weak Hamiltonian for weak nonleptonic hyperon and kaon decays (see Chapter II) transforms as $(8_L, 1_R)+(27_L, 1_R)$ under chiral $SU(3)_L \times SU(3)_R$. The octet part of the Hamiltonian dominates the rate for hyperon and kaon decays [f1]

In terms of the field $\Sigma(x)$ the $(8_L,1_R)$ piece of the effective Hamiltonian for weak nonleptonic kaon and hyperon decays is given by

$$H_{eff}^{\Delta S=1} = a \int d^3x \, Tr\, O \partial_\mu \Sigma \partial^\mu \Sigma^\dagger + \cdots , \tag{7.6}$$

where the ellipses represent terms with more than two derivatives, a is a constant and O is the matrix

$$O = \begin{pmatrix} 0 & 0 & 0 \\ 0 & 0 & 1 \\ 0 & 0 & 0 \end{pmatrix}. \tag{7.7}$$

Chiral perturbation theory relates the S-wave hyperon decay amplitudes to matrix elements of the effective Hamiltonian (7.6) between baryon states at zero momentum. These are determined by the two reduced matrix elements

$$\langle B_f | H_{eff}^{\Delta S=1} | B_i \rangle = D\, tr(B_f^\dagger \{B_i, O\}) - F\, tr(B_f^\dagger [B_i, O]), \tag{7.8}$$

using $SU(3)_V$ symmetry. Here B is the baryon matrix (6.4) of two component nonrelativistic spinors.

[f1] In the semiclassical approximation the $\Delta I=\frac{1}{2}$ rule for kaons does not necessarily imply one for hyperons. Higher derivative operators in the $(27_L,1_R)$ that are suppressed for kaon decays are not restricted to be negligible for hyperon decays.

Using the semiclassical approximation the F/D ratio can be predicted. In this approximation time derivatives in the effective Hamiltonian are neglected and

$$H_{eff}^{\Delta S=1} = -\int d^3x a[tr(A^\dagger OA\partial_j\Sigma_0\partial_j\Sigma_0^\dagger)+\cdots] \tag{7.9}$$

with Σ_0 defined in (7.2) . The spatial derivatives acting on Σ_0 give 3×3 matrices with zeros everywhere except in the upper 2×2 block. Any 2×2 matrix can be written as a linear combination of the identity and the Pauli matrices. Therefore, after integrating over space we obtain

$$H_{eff}^{\Delta S=1} \sim tr(\lambda^8 A^\dagger OA). \tag{7.10}$$

Here we have expressed the 2×2 identity matrix as a linear combination of λ^8 and the 3×3 identity matrix and used the tracelessness of $A^\dagger OA$. Note that this form for the effective action depends only on neglecting time derivatives and is valid to all orders in spatial derivatives.

Using the wave functions for the baryon octet we therefore have

$$\langle B_f|H_{eff}^{\Delta S=1}|B_i\rangle \sim \int dA\ D^{(8)*}_{a_f b_f}(A)D^{(8)}_{ab}D^{(8)}_{a_i b_i}(A), \tag{7.11a}$$

where

$$a = (1,\tfrac{1}{2},\tfrac{1}{2}), \tag{7.11b}$$

$$b = (0,0,0). \tag{7.11c}$$

This integral over group space can be expressed as a sum over products of Clebsch-Gordan coefficients [38] :

$$\langle B_f | H_{eff}^{\Delta S=1} | B_i \rangle \sim \sum_n \begin{pmatrix} 8 & 8 & 8 \\ a & a_i & a_f \end{pmatrix} \begin{pmatrix} 8 & 8 & n \\ b & b_i & b_f \end{pmatrix}. \tag{7.12}$$

In the sum over representations n, only the the two octets contribute. Using (7.12) we find that

$$\frac{F}{D} = -\frac{5}{3}. \tag{7.13}$$

This agrees, at the 20% level, with the experimental data on S-wave decays. The prediction in (7.13) gets corrections from operators in the effective Hamiltonian with one-time derivative.

3. *F/ D* for semileptonic hyperon decays.

The semileptonic hyperon decays and neutron β decay are determined by matrix elements of the axial current between baryon states at rest. $SU(3)_V$ symmetry implies that these matrix elements are parameterized by two quantities which we again denote by F and D.

$$<B_f|\int d^3x A_j^a(x)|B_i> = D\, tr(B_f^\dagger \sigma_j \{B_k,\lambda_a\}) - F\, tr(B_f^\dagger \sigma_j [B_i,\lambda^a]). \quad (7.14)$$

The relevant component for weak semileptonic hyperon decays is $a = 4+i5$ since

$$\lambda^{4+i5} = \begin{pmatrix} 0 & 0 & 1 \\ 0 & 0 & 0 \\ 0 & 0 & 0 \end{pmatrix} \quad (7.15)$$

corresponds to changing a strange quark to an up quark.

In the semiclassical approximation the same techniques that were used in the previous Section give

$$\int d^3a A_i^a(x) \sim tr[\lambda^i A^\dagger \lambda^a A] \quad (7.16)$$

and so, for example,

$$<B_f|\int d^3x A_3^{4+i5}(x)|B_i> \sim \int dA\; D^{(8)*}_{a_f b_f}(A) D^{(8)}_{ab} D^{(8)}_{a_i b_i}(A), \quad (7.17a)$$

where

$$a = (1,\tfrac{1}{2},\tfrac{1}{2}), \quad (7.17b)$$

$$b = (0,1,0). \quad (7.17c)$$

Expressing the integral over group space in (7.17a) as a sum over products of Clebsch-Gordan coefficients we find that

$$\frac{F}{D} = \frac{5}{9}. \tag{7.18}$$

This agrees extremely well with the experimental value $F/D = 0.54$ [27]. The nonrelativistic quark model with static $SU(6)$ wave functions predicts $F/D = 2/3$.

Our semiclassical prediction for F/D gets corrections from operators in the axial current with a single time derivative.

4. F/D for hyperon magnetic moments.

The magnetic moments of hyperons and nucleons are determined from matrix elements of the magnetic moment operator

$$\mu_j = \frac{1}{2}\int d^3x\, \varepsilon_{jkl} x_k J_l^{em}(x). \tag{7.19}$$

The electromagnetic current transforms like an octet under $SU(3)_V$. Therefore, matrix elements of μ_j between hyperons and nucleons are parameterized by two quantities which we again denote by F and D.

$$\langle B_f|\mu_j|B_i\rangle = D\, tr(B_f^\dagger \sigma_j \{B_i, Q\}) - F\, tr(B_f^\dagger \sigma_j [B_i, Q]). \tag{7.20}$$

Here Q is the quark-charge generator

$$Q = \begin{pmatrix} \frac{2}{3} & 0 & 0 \\ 0 & -\frac{1}{3} & 0 \\ 0 & 0 & -\frac{1}{3} \end{pmatrix}. \tag{7.21}$$

The magnetic moment operator is the integral of an axial current over space and in the semiclassical approximation

$$\mu_i \sim tr[\lambda^i A^\dagger Q A]. \tag{7.22}$$

This gives

$$\frac{F}{D} = \frac{5}{9} \tag{7.23}$$

just as in the case of the axial current couplings relevant for semileptonic hyperon decays. Our predictions for magnetic moments agree with experiments at the 50% level. However, pure $SU(3)_V$ predictions for

magnetic moments are not much better. One-loop corrections for magnetic moments are rather large[17].

Predictions for magnetic moments including operators with one-time derivative can be found in [39].

VIII. CONCLUSION.

In this work we derived the low-energy effective weak Hamiltonian for $\Delta S=1$ decays expressed in quark fields. We reviewed chiral perturbation theory to lowest-order and explained how parts of the higher-order corrections can be uniquely determined from loop diagrams involving only the lowest-order operators.

Using chiral perturbation theory, we calculated those higher-order corrections for a variety of processes. We found that the application of chiral perturbation theory to $K^0\bar{K}^0$ mixing is unreliable. This had consequences for a number of predictions made in the literature using chiral perturbation theory in the $K^0\bar{K}^0$ system [19].

It was also found that $K\pi\pi$ matrix elements can be reliably obtained from $K\pi$ and K-vacuum matrix elements. This allows to verify $\Delta I=1/2$ enhancement in lattice calculations of the latter matrix elements.

Some applications of chiral perturbation theory to hyperon properties were reviewed and the next-to-leading corrections were calculated. We found that the lowest-order relations for masses and semileptonic decays didn't receive large corrections. However, the corrections to nonleptonic P-wave decays and to one S-wave decay were large. The vanishing of $A^{(S)}(\Sigma^+\to n\pi^+)$ remained true in the next-to-leading order, but the large correction to $A^{(S)}(\Xi^-\to\Lambda\pi^-)$ invalidated the Lee-Sugawara relation. The large corrections to the P-wave decays explain the discrepancy between experiments and the lowest-order predictions.

In the soliton model for baryons, we derived some relations that are independent of the specific model for mesons used. These predictions

provided a test for the semiclassical expansion used in the soliton model. For the predictions we calculated, the agreement with experiments was at about the same level as the pure $SU(3)_V$ predictions.

Appendix A : Definition of Z and Δm^2.

The definition of field renormalization and mass renormalization is given here for a real scalar field, but we use the generalization to complex scalars and fermions in the text.

The quadratic part of the bare Lagrangian is given by

$$L_B=\tfrac{1}{2}\partial_\mu\varphi\partial^\mu\varphi-\tfrac{1}{2}m_B^2\varphi^2 \tag{A.1}$$

and for p^2 near the physical mass the propagator is given by

$$iG_0=\frac{iZ}{p^2-m_{ph}^2} \tag{A.2}$$

where m_{ph} is the physical particle mass.

The propagator calculated using perturbation theory to one-loop is, with $i\alpha p^2+i\beta$ the one-loop contribution without external propagators,

$$iG_0=\frac{i}{p^2-m_B^2}+\frac{i}{p^2-m_B^2}(i\alpha p^2+i\beta)\frac{i}{p^2-m_B^2}. \tag{A.3}$$

Treating α, β and $Z-1$ as small, this leads to

$$Z(p^2-m_B^2)+\alpha p^2+\beta=p^2-m_{ph}^2. \tag{A.4}$$

So at this level of perturbation theory we have

$$Z = 1-\alpha \tag{A.5}$$

$$\begin{aligned} m_{ph}^2 &= m_B^2+\Delta m^2 \\ &= m_B^2 + (Z-1)m_B^2 - \beta. \end{aligned} \tag{A.6}$$

Appendix B : Integrals.

To evaluate the integrals needed we use dimensional regularization. Since we know [12] that all infinite contributions cancel against contributions from higher-dimension operators we are interested only in finite parts. Of these finite parts the parts depending analytically on the mass parameters (m^2, q^2) are undetermined, too, because they can get contributions from higher-dimension operators.

As an example of the extraction of a nonanalytic part we evaluate (3.27).

$$\int \frac{d^{4-\varepsilon}p}{(2\pi)^{4-\varepsilon}} \frac{1}{p^2-m^2} = \frac{-i\Gamma(-1+\frac{\varepsilon}{2})}{(4\pi)^{2-\frac{\varepsilon}{2}}} (m^2)^{1-\frac{\varepsilon}{2}}. \tag{B.1}$$

The only nonanalytic dependence on masses here is in $m^{-\varepsilon}$. Using the expansion of the Γ function and

$$m^{-\varepsilon} \approx 1-\varepsilon \log m, \tag{B.2}$$

we get

$$\int \frac{d^4p}{(2\pi)^4} \frac{1}{p^2-m^2} = \frac{-i}{16\pi^2} \log m^2. \tag{B.3}$$

Including the μ dependence of vertices leads then to

$$\int \frac{d^4p}{(2\pi)^4} \frac{1}{p^2-m^2} = \frac{-i}{16\pi^2} \log \frac{m^2}{\mu^2}. \tag{B.4}$$

References.

[1] S. Weinberg, Phys. Rev. Lett. 19(1967)1264;

A. Salam, in : Elementary Particle Theory : Relativistic Groups and Analyticity, Nobel Symposium No. 8, ed. N. Svartholm, Almquist and Wicksell, Stockholm, 1968, p. 367.

[2] M. Kobayashi and T. Maskawa, Prog. Theor. Phys. 49(1973)652.

[3] F. Gilman and M. Wise, Phys. Rev. D20(1979)2392;

B. Guberina and R. Peccei, Nucl. Phys. B163(1980)289.

[4] F. Gilman and M. Wise, Phys. Rev. D27(1983)1128.

[5] J. Bijnens and M. Wise, Phys. Lett. 137B(1984)245.

[6] E. Witten, Nucl. Phys. B122(1977)109.

[7] F. Gilman and M. Wise, Phys. Rev. D21(1980)3150.

[8] M. Peskin, lectures in Les Houches Summer Institute, 1982, SLAC-PUB-3021.

[9] S. Coleman et al., Phys. Rev. 177(1969)2239;

C. Callan et al., Phys. Rev. 177(1969)2247.

[10] A. Manohar and H. Georgi, Nucl. Phys. B234(1984)189.

[11] S. Treiman et al., Lectures on Current Algebra and its Applications, Princeton University Press, Princeton, 1972.

[12] S. Weinberg, Physica 96A(1979)327.

[13] H. Georgi, Weak Interaction and Modern Particle Theory, Benjamin-Cummings, Menlo Park, 1984.

[14] L.-F. Li and H. Pagels, Phys. Rev. D5(1972)1509.

[15] P. Langacker and H. Pagels, Phys. Rev. D8(1973)4595.

[16] P. Langacker and H. Pagels, Phys. Rev. D10(1974)2904.

[17] D. Caldi and H. Pagels, Phys. Rev. D10(1974)3739.

[18] A. Cohen and A. Manohar, Phys. Lett. 143B(1984)481.

[19] M. Wise, talk at SLAC Summer Institute on Particle Physics, 1984, CALT-68-1179 and references therein.

[20] T.D. Lee and C.S. Wu, Ann. Rev. Nucl. Sc. 16(1966)511.

[21] R. Crewther et al., Phys. Lett. 88B(1979)123.

[22] J. Donoghue et al., Phys. Lett. 119B(1982)311.

[23] J. Bijnens et al., Phys. Rev. Lett. 53(1984)2367.

[24] M. Gaillard and B. Lee, Phys. Rev. Lett. 33(1974) 108.

[25] N. Cabibbo et al., Rome-382-1983.

R. Brower et al., Phys. Rev. Lett. 53(1984)1318.

[26] C. Bernard et al.,CALT-68-1211; UCLA/84/TEP/14.

[27] J. Bijnens, Phys. Lett. 152B(1985)226.

[28] M. Gell-Mann, Caltech Report CTSL-20 (1961) unpublished.

S. Okubo, Prog. Theor. Phys. (Kyoto) 27(1962)949.

[29] R. Schrock and L. Wang, Phys. Rev. Lett. 41(1978)692.

[30] J. Bijnens et al., CALT-68-1221.

[31] See for example, D. Bailin, Weak Interactions, Adam Hilger Ltd., Bristol, 1982.

[32] B. Lee, Phys. Rev. Lett. 12(1964)83.

H. Sugawara, Prog. Theor. Phys. 31(1964)213.

[33] T. Skyrme, Proc. Roy. Soc. A260(1961)270.

[34] J. Wess and B. Zumino, Phys. Lett. 37B(1971)95.

E. Witten, Nucl. Phys. B223(1983)422.

[35] E. Witten, Nucl. Phys. B223(1983)433.

A. Balachandran et al.,Phys. Rev. Lett. 49(1982)1124.

[37] E. Witten, Nucl. Phys. B160(1979)57.

[37] E. Guadagnini, Nucl. Phys. B236(1984)35.

[38] J. De Swart, Rev. Mod. Phys. 35(1963)916.

S. McNamee and F. Chilton, Rev. Mod. Phys. 36(1964)1005.

[39] G. Adkins and C. Nappi, Nucl. Phys. B249(1985)507.

[40] J. Bijnens et al., Phys. Lett. 140B(1984)421.

List of Tables

Table 1

Coefficients of the $\Delta S=1$ Hamiltonian. τ is given by

$$\tau = s_2^2 + \frac{s_2 c_2 s_3 e^{-i\delta}}{c_1 c_3}.$$

table 1 : Coefficients of the $\Delta S=1$ Hamiltonian		
Λ''^2	0.01 GeV^2	0.1 GeV^2
C_1	$-0.99 + 0.033\tau$	$-0.93 + 0.049\tau$
C_2	$1.60 - 0.033\tau$	$1.55 - 0.049\tau$
C_3	$-0.033 - 0.006\tau$	$-0.022 - 0.014\tau$
C_5	$0.018 + 0.004\tau$	$0.011 + 0.009\tau$
C_6	$-0.099 - 0.099\tau$	$-0.048 - 0.01\ \tau$
C_7	$(0.037 - 0.067\tau)\alpha_{em}$	$(0.025 - 0.048\tau)\alpha_{em}$
C_8	$(0.008 - 0.11\ \tau)\alpha_{em}$	$(0.004 - 0.06\ \tau)\alpha_{em}$

Table 2

Coefficients of the ΔS=2 Hamiltonian.

table 2. Coefficients of ΔS=2 Hamiltonian		
Λ''^2	0.01 GeV^2	0.1 GeV^2
η_1	0.69	0.99
η_2	0.59	0.60
η_3	0.41	0.40

Table 3

The hyperon decay amplitudes $A^{(S)}$, $A^{(P)}$ measured in the unit of $G_F m_{\pi^+}^2$. $D = .81$, $F = .44$, $a = .56 G_F m_{\pi^+}^2 f_\pi$, $b = -1.42\, G_F m_{\pi^+}^2 f_\pi$, $\mu = 1\, GeV$ are used for calculation.

mode	$A_{exp.}^{(S)}$	$A_{in}^{(S)}$ (6.31)	$\Delta A_{in}^{(S)}$ (6.35)	$A_{exp.}^{(P)}$	$A_{in}^{(P)}$ (6.32)	$\Delta A_{in}^{(P)}$ (6.38)
$\Sigma^+ \to n\pi^+$	.06 ± .01	0	0	19.07 ± .07	1.3	-4.8
$\Sigma^- \to n\pi^-$	1.93 ± .01	2.0	-.6	−.65±.07	-4.2	-3.1
$\Lambda \to p\pi^-$	1.47±.01	1.5	.3	9.98±.24	10.4	9.0
$\Xi^- \to \Lambda\pi^-$	−2.04±.01	-2.0	1.5	7.49±.28	-1.8	-9.7

Figure Captions

1. Weak decays mediated by one W exchange.
2. Penguin Diagram.
3. 1PI one-loop diagrams for four fermion operators.
4. Diagram for the decay $K^0 \to \pi^0\pi^0$.
5. Diagrams for the decay $K^0 \to \pi^0\pi^0\pi^0$.
6. Diagram for meson field renormalization and meson mass renormalization.
7. One-loop diagram for evaluation of f_π.
8. One-loop diagrams for $<\bar{K}^0|O^{(27)}|K^0>$.
9. One-loop diagrams for $<\pi^+\pi^0|O^{(27)}|K^0>$.
10. One-loop diagrams for $<\pi^0\pi^0|O^{(8)},O^{(27)}|K^0>$.
11. One-loop diagram for $<o|O^{(8)},O'|K^0>$.
12. One-loop diagram for $<\pi^0|O^{(8)},O^{(27)},O'|K^0>$.
13. One-loop diagram for $<o|j_\mu^{L1+i2}|\pi^+>$.
14. Feynman diagrams that give contributions of order $m_s \ln m_s$ to the matrix elements of the axial current. Here a circled "x" is an insertion of the axial current and a darkened circle is a strong interaction vertex from the Lagrangian density in eq. (6.9).
15. Feynman diagrams that give contributions of order $m_s^{3/2}$ and $m_s^2 \ln m_s$ to the baryon masses. Here a shaded triangle is a strong interaction vertex from the Lagrangian density in eq. (6.11) and a shaded circle is a strong interaction vertex from the Lagrangian density in eq. (6.9). Fig. (15a) contributes directly to baryon

masses while Fig. (15b) contributes directly to baryon masses and indirectly through wave function renormalization.

16. Pole diagrams responsible for leading contribution to P-wave hyperon decay amplitudes. In Fig. (16) a shaded square is a weak interaction vertex from (6.27) and a shaded circle is a strong interaction vertex from (6.9).

17. One-loop Feynman diagrams that give a nonzero contribution of order $m_s \ln m_s$ to the S-wave nonleptonic hyperon decay amplitudes. Here a shaded square is a weak interaction vertex from (6.27) and a shaded circle is a strong interaction vertex from (6.9).

18. One-loop Feynman diagrams that give a nonzero contribution of order $m_s \ln m_s$ to the P-wave nonleptonic hyperon decay amplitudes. In Figs. (18) a shaded square is a weak interaction vertex from (6.27) and a shaded circle is a strong interaction vertex from (6.9).

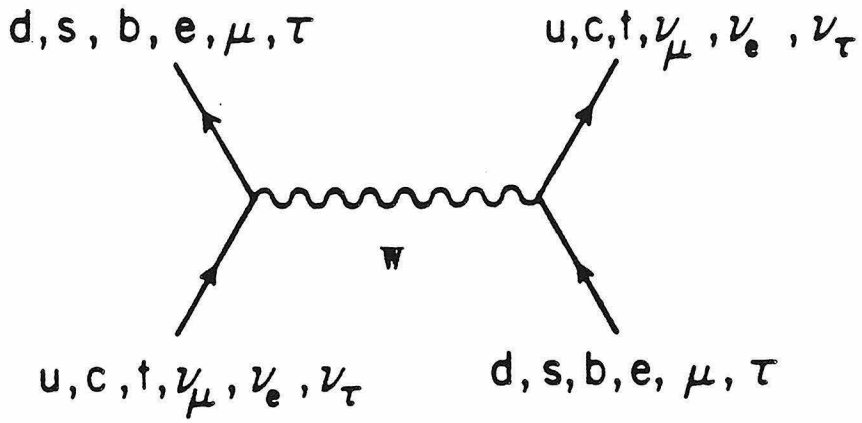

Figure (1)

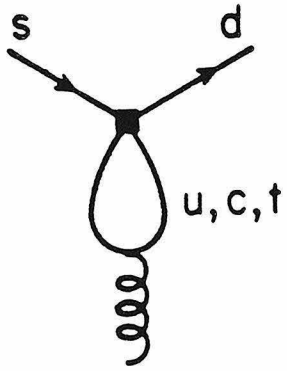

Figure (2)

Figure (3)

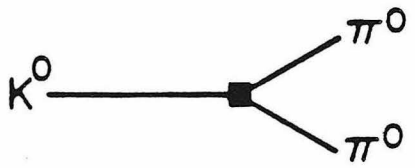

Figure (4)

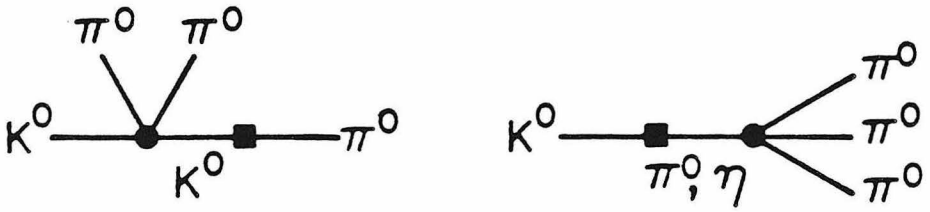

(a) (b)

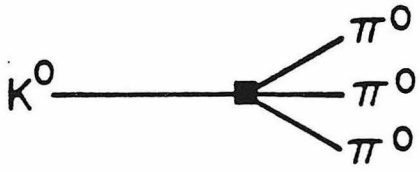

(c)

Figure (5)

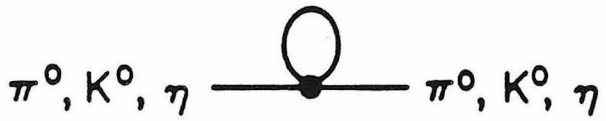

Figure (6)

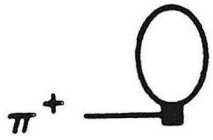

Figure (7)

(a) (b)

Figure (8)

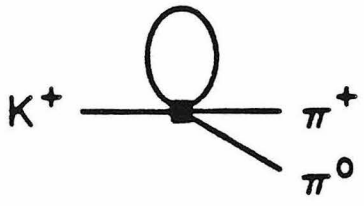

(a)

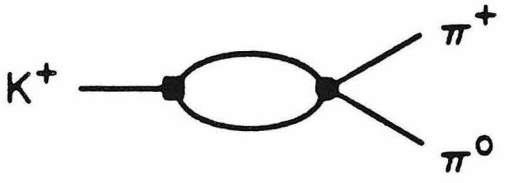

(b)

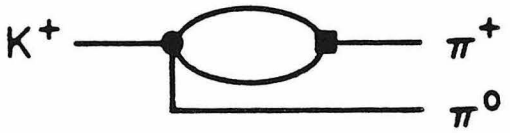

(c)

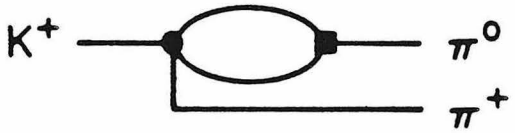

(d)

Figure (9)

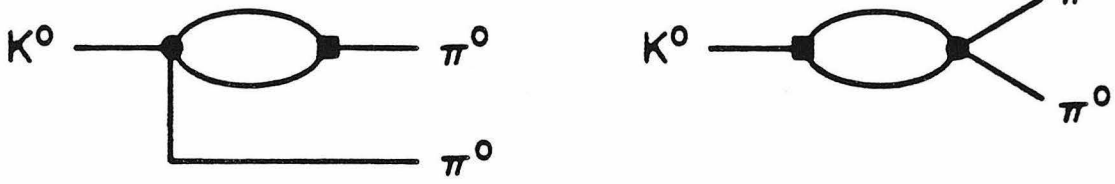

(a) (b)

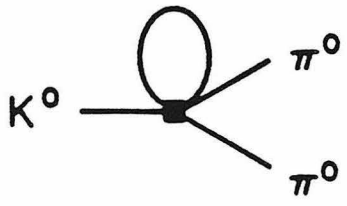

(c)

Figure (10)

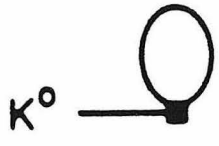

Figure (11)

(a) (b)

Figure (12)

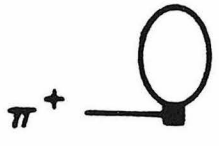

Figure (13)

Figure (14)

Figure (15)

Figure (16)

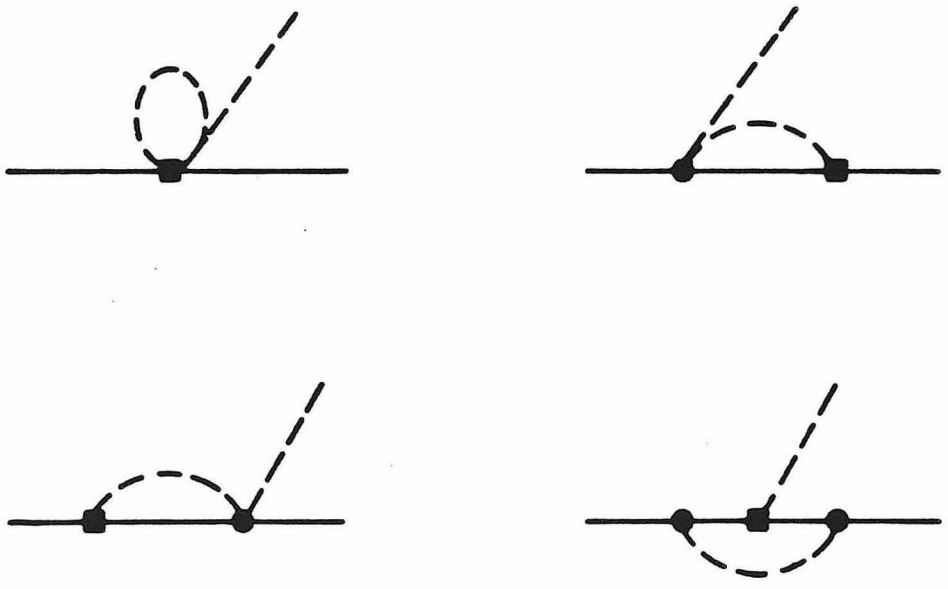

Figure (17)

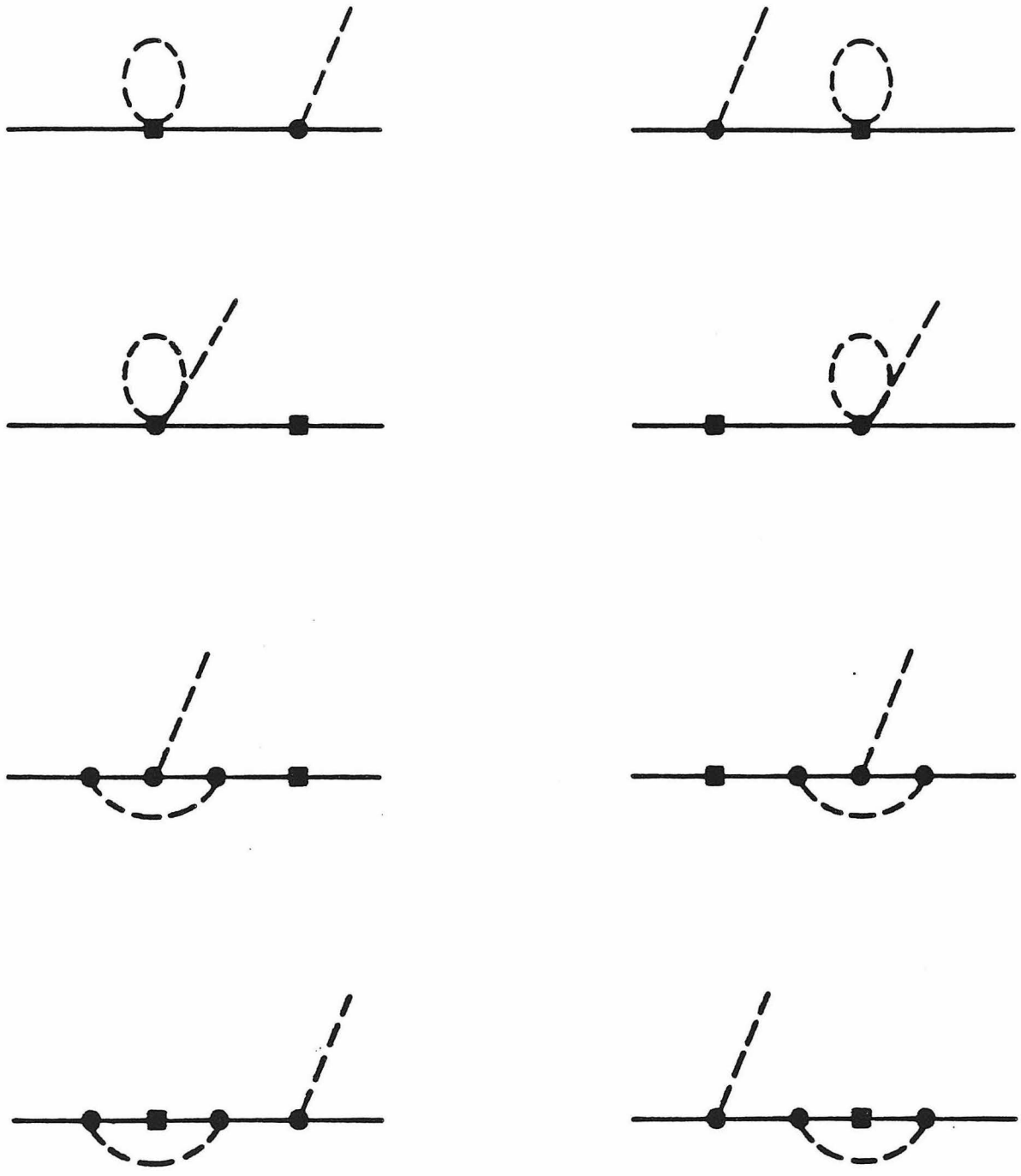

Figure (18)